

# Characterization of two conserved cell death elicitor families from the Dothideomycete fungal pathogens *Dothistroma septosporum* and *Fulvia fulva* (syn. *Cladosporium fulvum*)

1 Mariana Tarallo<sup>1,\*</sup>, Rebecca L. McDougal<sup>2</sup>, Zhiyuan Chen<sup>3</sup>, Yan Wang<sup>3</sup>, Rosie E. Bradshaw<sup>1,\*</sup>,  
2 Carl H. Mesarich<sup>4,\*</sup>

3 <sup>1</sup>Laboratory of Molecular Plant Pathology/Bioprotection Aotearoa, School of Natural Sciences,  
4 Massey University, Private Bag 11222, Palmerston North 4442, New Zealand

5 <sup>2</sup>Scion, Titokorangi Drive, Private Bag 3020, Rotorua 3046, New Zealand

6 <sup>3</sup>Department of Plant Pathology, Nanjing Agricultural University 210095, Nanjing, China

7 <sup>4</sup>Laboratory of Molecular Plant Pathology/Bioprotection Aotearoa, School of Agriculture and  
8 Environment, Massey University, Private Bag 11222, Palmerston North 4442, New Zealand

## 9 \*Correspondence:

10 Corresponding authors: M. Tarallo (m.tarallo@massey.ac.nz), R. E. Bradshaw  
11 (r.e.brashaw@massey.ac.nz) and C. H. Mesarich (c.mesarich@massey.ac.nz)

12

13 **Keywords:** Dothideomycetes, cell death-eliciting effectors, protein families, immune receptors,  
14 plant-pathogen interactions, protein tertiary structure.

## 15 Abstract

16 *Dothistroma septosporum* (Ds) and *Fulvia fulva* (Ff; previously called *Cladosporium fulvum*) are two  
17 closely related Dothideomycete fungal species that cause Dothistroma needle blight in pine and leaf  
18 mold in tomato, respectively. During host colonization, these pathogens secrete virulence factors  
19 termed effectors to promote infection. In the presence of corresponding host immune receptors,  
20 however, these effectors activate plant defenses, including a localized cell death response that halts  
21 pathogen growth. We identified two effector protein families, Ecp20 and Ecp32, which are conserved  
22 between the two pathogens. The Ecp20 family has four paralogues in both species, while the Ecp32  
23 family has four paralogues in *D. septosporum* and five in *F. fulva*. Both families have members that  
24 are highly expressed during host infection. Members of the Ecp20 family have predicted structural  
25 similarity to proteins with a  $\beta$ -barrel fold, including the Alt a 1 allergen from *Alternaria alternata*,  
26 while members of the Ecp32 family have predicted structural similarity to proteins with a  $\beta$ -trefoil  
27 fold, such as trypsin inhibitors and lectins. Using *Agrobacterium tumefaciens*-mediated transient  
28 transformation assays, each family member was assessed for its ability to trigger cell death in leaves  
29 of the non-host species *Nicotiana benthamiana* and *N. tabacum*. Using this approach, FfEcp20-2,  
30 DsEcp20-3 and FfEcp20-3 from the Ecp20 family, and all members from the Ecp32 family, except  
31 for the Ds/FfEcp32-4 pair, triggered cell death in both species. This cell death was dependent on  
32 secretion of the effectors to the apoplast. In line with recognition by an extracellular immune  
33 receptor, cell death triggered by Ds/FfEcp20-3 and FfEcp32-3 was compromised in *N. benthamiana*  
34 silenced for *BAK1* or *SOBIR1*, which encode extracellular co-receptors involved in transducing  
35 defense response signals following apoplastic effector recognition. We then investigated whether  
36 DsEcp20-3 and DsEcp20-4 triggered cell death in the host species *Pinus radiata* by directly  
37 infiltrating purified protein into pine needles. Strikingly, as in the non-host species, DsEcp20-3

38 triggered cell death, while DsEcp20-4 did not. Collectively, our study describes two new candidate  
39 effector families with cell death-eliciting activity from *D. septosporum* and *F. fulva* and provides  
40 evidence that members of these families are recognized by plant immune receptors.

41 **1 Introduction**

42 Understanding how plants and fungal pathogens interact at the molecular level can lead to  
43 improvements in plant health. During infection, fungal pathogens deliver a collection of small,  
44 proteinaceous virulence factors, termed effectors, into the apoplast and/or cells of their host plants to  
45 promote the infection process (Rocafort et al., 2020; Wang et al., 2020). However, as fungal infection  
46 has a negative impact on plant fitness, there is a strong selection pressure on the host to recognize  
47 these effectors as invasion patterns and, in doing so, activate defense responses that provide  
48 protection against the pathogen (Cook et al., 2015) In line with this, in resistant hosts, particular  
49 effectors may be recognized by corresponding specific immune receptors, called resistance (R)  
50 proteins, to activate plant defense responses. Often, one of these defense responses is the  
51 hypersensitive response (HR), a localized cell death reaction that limits or halts pathogen growth  
52 (Cook et al., 2015; Win et al., 2012). As these defense responses often lead to the pathogen being  
53 unable to cause disease, such recognized effectors are typically referred to as avirulence (Avr)  
54 determinants. To circumvent recognition, and therefore the ensuing plant defense responses, the  
55 fungal invader must then modify its effector arsenal by secreting mutated or new effectors, shifting  
56 the pressure to adapt back onto the plant host, resulting in a constant "arms race" in plant-pathogen  
57 interactions (Coll et al., 2011; Jones & Dangl, 2006).

58 Progress in the generation of genomic, transcriptomic, and proteomic resources has enabled the rapid  
59 identification of pathogen effectors, making it possible to screen them for elicitation or suppression  
60 of plant defense responses, a process known as effectoromics. This, in turn, makes it possible to  
61 discover host defense or susceptibility genes in different plant species. A search for conserved  
62 effectors, sometimes called 'core' effectors, is essential as it can lead to broad spectrum resistance.  
63 The tertiary structures of some effector proteins are conserved across microbial classes because they  
64 have fundamental and important roles in infection, and for this reason are less likely to be mutated or  
65 lost during microbial evolution (Nürnberg & Brunner, 2002). Therefore, plant resistance based on  
66 the recognition of conserved effectors is more likely to be durable, as it is less likely to be overcome.

67 *Dothistroma septosporum* (Ds) is a hemibiotrophic pathogen that causes Dothistroma needle blight  
68 (DNB), one of the most important foliar diseases of pine trees (Drenkhan et al., 2016). Based on  
69 genomic information, *D. septosporum* is closely related to *Fulvia fulva* (Ff; syn. *Cladosporium*  
70 *fulvum*) (de Wit et al., 2012). *F. fulva* is a biotrophic pathogen responsible for leaf mold of tomato  
71 (*Solanum lycopersicum*), a disease that is mainly a problem in greenhouse or high tunnel  
72 environments (Thomma et al., 2005). In both the *D. septosporum*-pine and *F. fulva*-tomato  
73 pathosystems, infection begins with the germination of conidia on the leaf surface and penetration of  
74 hyphae into the host through the stomata. Once inside, both pathogens colonize the apoplastic space  
75 between mesophyll cells, where they secrete effector proteins (Kabir et al., 2015; Mesarich et al.,  
76 2018).

77 *F. fulva* is one of the best studied filamentous fungal pathogens. The *F. fulva*-tomato interaction is a  
78 model pathosystem in which early pioneering studies helped to establish the molecular basis of the  
79 gene-for-gene concept of plant resistance to fungal pathogens (de Wit, 2016). In *F. fulva*, small,  
80 secreted cysteine-rich proteins delivered to the host apoplast, termed extracellular proteins (Ecps)  
81 based on their identification in apoplastic wash fluid samples, have been well-studied (Mesarich et

82 al., 2018). These include core effectors such as Ecp2-1, Ecp6 and Avr4 (de Jonge et al., 2010;  
83 Sánchez-Vallet et al., 2013; Stergiopoulos et al., 2010; van den Burg et al., 2006), homologs of which  
84 have been found in other plant-pathogenic fungi, including *D. septosporum* (Bolton et al., 2008; de  
85 Wit et al., 2012; Stergiopoulos et al., 2012). In contrast, few studies have identified and characterized  
86 effectors from *D. septosporum*. In one of these studies, DsEcp2-1, the ortholog of Ecp2-1 from *F.*  
87 *fulva*, was suggested to be an Avr protein responsible for eliciting defense responses in pine (Guo et  
88 al., 2020). In another of these studies, DsAvr4, the ortholog of Avr4 from *F. fulva*, was found to bind  
89 chitin, a function that is required to protect the fungal cell wall against hydrolysis by host chitinases  
90 (Mesarich et al., 2016; van den Burg et al., 2006).

91 In general, studies highlighting the role of effectors in molecular interactions between pathogens and  
92 gymnosperm hosts are few and far between. The close phylogenetic relationship between *D.*  
93 *septosporum* and *F. fulva*, however, provides a unique opportunity for comparative analysis of core  
94 effector functions across angiosperm and gymnosperm pathosystems. Recently, a set of candidate  
95 effector proteins from *D. septosporum* was transiently expressed in the non-host plants, *Nicotiana*  
96 *benthamiana* and *N. tabacum*, to identify those that are involved in triggering plant defense responses  
97 (Hunziker et al., 2021). Several of these proteins, all with orthologs in *F. fulva*, elicited a plant cell  
98 death response, suggesting that they are recognized by extracellular immune receptors in these non-  
99 host plants, triggering non-host resistance. Amongst these we found two proteins, Ds70057 and  
100 Ds70694, that were of particular interest, as they are orthologs of Ecps from *F. fulva* (Hunziker et al.,  
101 2021; Mesarich et al., 2018). Both proteins appear to be part of protein families – the Ecp20 family  
102 and the Ecp32 family (Hunziker et al., 2021). The Ecp20 family is made up of four members in both  
103 species, while the Ecp32 family is made up of four members in *D. septosporum* and five members in  
104 *F. fulva*.

105 In this study, we characterized and compared Ecp20 and Ecp32 family members from *D.*  
106 *septosporum* and *F. fulva* through prediction of their protein tertiary structures and by assessing their  
107 cell death-eliciting capacity in non-host angiosperm plants. We also used a novel assay involving a  
108 pine tissue culture system to determine whether two of the Ecp20 family members from *D.*  
109 *septosporum* trigger cell death in the gymnosperm host, *Pinus radiata*. This work provides insights  
110 into conservation of core effector function and recognition across a broad range of plant species.

## 111 2 Methods

### 112 2.1 Microorganisms and Plants

113 *D. septosporum* NZE10 (de Wit et al., 2012), GUA2 and COLN (Bradshaw et al., 2019), as well as  
114 *D. pini* CBS 116487 (BioSample ID SAMN02254964) and *F. fulva* 0WU (de Wit et al., 2012), were  
115 used to identify candidate effectors for characterization in this study. *Escherichia coli* DH5 $\alpha$  (Taylor  
116 et al., 1993) and *Agrobacterium tumefaciens* GV3101 (Holsters et al., 1980) were used for gene  
117 cloning and *A. tumefaciens*-mediated transient transformation assays (ATTAs), respectively. *N.*  
118 *tabacum* Wisconsin 38 and *N. benthamiana* were used as model non-host plants for ATTAs, while *N.*  
119 *benthamiana* was used for tobacco rattle virus (TRV)-mediated gene silencing experiments. *P.*  
120 *radiata* clonal shoots, derived from family seed lots that are, compared to each other, relatively  
121 susceptible (S6 and S11) or tolerant (R4) to DNB, and grown from embryogenic tissue under sterile  
122 conditions on LPch agar (Hargreaves et al., 2004), were provided by Scion (New Zealand Forest  
123 Research Institute Ltd., Rotorua, New Zealand) and used in protein infiltration assays.

### 124 2.2 Bioinformatics

125 Members of the Ecp20 and Ecp32 protein families were identified from the predicted proteomes  
126 and/or genomes of *D. septosporum* NZE10 and *F. fulva* 0WU (de Wit et al., 2012). Chromosome  
127 locations of the *FfEcp20* and *FfEcp32* genes were identified using the *F. fulva* Race 5 genome  
128 assembly (Zaccaron et al., 2022). Gene family members were also identified from genome sequences  
129 of 18 other *D. septosporum* isolates (Bradshaw et al., 2019) and *D. pini* CBS 116487 (GenBank  
130 assembly accession GCA\_002116355.1), using reciprocal BLASTp and tBLASTn searches in  
131 conjunction with an E-value cut-off of  $<10^{-5}$ . BLASTp was also employed to determine the level of  
132 conservation for each family member across fungal species in the Joint Genome Institute (JGI)  
133 MycoCosm database, using an E-value threshold of  $10^{-5}$ . EffectorP v3.0 (Sperschneider & Dodds,  
134 2021) was used to predict whether members of the Ecp20 and Ecp32 families are effectors. All *D.*  
135 *septosporum* NZE10, *D. pini* CBS 116487 and *F. fulva* 0WU nucleotide and amino acid sequences  
136 for Ecp20 and Ecp32 family members are shown in Supplementary Table S1.

137 Protein tertiary structure predictions were performed using AlphaFold2 (Jumper et al., 2021; Mirdita  
138 et al., 2022), and the Dali server (Holm, 2020) was used to identify proteins with structural similarity  
139 in the Research Collaboratory for Structural Bioinformatics Protein Data Bank (RCSB PDB). Here, a  
140 Dali Z-score of 2 or greater was used to infer structural similarity. Protein tertiary structures were  
141 visualized and rendered in PyMol v2.5, with alignments carried out using the CEalign tool (DeLano,  
142 2002).

143 Protein sequence alignments were performed using Clustal  $\Omega$  (Sievers et al., 2011) in Jalview  
144 ([www.jalview.org](http://www.jalview.org)). Phylogenetic trees were constructed with the neighbor-joining method using  
145 Geneious Software v9.1.8 (Kearse et al., 2012).

### 146 2.3 ATTA Expression Vectors

147 Candidate effector genes of *D. septosporum* NZE10, GUA2 and COLN, *D. pini* CBS 116487 and *F.*  
148 *fulva* 0WU were cloned in the pICH86988 ATTA expression vector, which contains the nucleotide  
149 sequence encoding the *N. tabacum* PR1 $\alpha$  signal peptide for secretion into the plant apoplast, followed  
150 by a 3 $\times$ FLAG for detection via Western blotting (Weber et al. (2011), according to the method  
151 described by Guo et al. (2020) in cases where the genes had no predicted introns, or synthesized  
152 directly into pICH86988 by Twist Bioscience (San Francisco, CA, USA) in cases where the genes  
153 had predicted introns. For the genes that were cloned into pICH86988, the mature coding sequence  
154 was first amplified by polymerase chain reaction (PCR) from genomic DNA extracted from the  
155 fungus, with genomic DNA extraction performed as described by Doyle and Doyle (1987). PCRs  
156 were performed with Phusion High-Fidelity DNA polymerase (New England Biolabs, Beverly, MA,  
157 USA), and PCR products were extracted from agarose gels using an E.Z.N.A.<sup>®</sup> Gel Extraction Kit  
158 (Omega Bio-tek, Norcross, GA, USA). PCR primers were designed with Primer3 (Untergasser et al.,  
159 2012) in Geneious v9.1.8 (Kearse et al., 2012). These primers, which were synthesized by Integrated  
160 DNA Technologies (IDT; Supplementary Table S2), had 5' extensions containing a BsaI recognition  
161 site and 4-base overhang specific for Golden Gate modular cloning (Engler et al., 2009) in between  
162 the CaMV 35S promoter and octopine synthase terminator of pICH86988. Versions of the candidate  
163 effector genes were also ligated into pICH86988 without the nucleotide sequence encoding the PR1 $\alpha$   
164 signal peptide to prevent secretion of the proteins they encode into the apoplast. Constructs were then  
165 transformed into *E. coli*, plasmids extracted using an E.Z.N.A.<sup>®</sup> Plasmid DNA Mini Kit I (Omega  
166 Bio-tek), and correct assemblies confirmed by sequencing. ATTA expression vectors were  
167 transformed into *A. tumefaciens* by electroporation as described previously (Guo et al., 2020).

### 168 2.4 ATTAs

169 To heterologously express candidate effector genes in *N. benthamiana* and *N. tabacum* using ATTAs,  
170 single colonies of *A. tumefaciens* carrying pICH86988 constructs of interest were first inoculated into  
171 selective lysogeny broth (LB) containing 50 µg/mL kanamycin, 10 µg/mL rifampicin and 30 µg/mL  
172 gentamycin, then incubated overnight at 28°C. Cells were subsequently collected by centrifugation at  
173 2,500 g for 5 min and resuspended in 1 mL of infiltration buffer (10 mM MgCl<sub>2</sub>:6H<sub>2</sub>O, 10 mM MES-  
174 KOH (Sigma-Aldrich, St. Louis, MO, USA), 100 µM acetosyringone (Sigma-Aldrich)) to an OD<sub>600</sub>  
175 of 0.5. Following resuspension, the abaxial surface of *N. benthamiana* and *N. tabacum* leaves was  
176 infiltrated with the appropriate *A. tumefaciens* suspension using 1 mL needleless syringes. Here, the  
177 extracellular elicitin INF1 from *Phytophthora infestans*, which is recognized by the LRK1 immune  
178 receptor in *Nicotiana* species (Kamoun et al., 1997; Kanzaki et al., 2008), was used as a positive cell  
179 death control, while the empty pICH86988 vector was used as a negative no cell death control. At  
180 least 12–24 infiltration zones were tested for each candidate effector gene or control (consisting of  
181 two leaves from each of two plants ×3–6 repeat experiments). Plants were monitored for up to 7 days,  
182 and photographs taken using a Nikon D7000 camera. Infiltration zones were assessed on whether the  
183 protein tested elicited a strong or weak cell death response, or no cell death. A strong cell death  
184 response was scored when it was indistinguishable from the response elicited by INF1 and around the  
185 entire infiltration zone, while a weak response was considered when the protein elicited a weaker  
186 response around approximately 50% of the infiltration zone when compared with INF1. A no-cell  
187 death response was indicated when the infiltration zone had the same response as the negative empty  
188 pICH86988 vector control.

## 189 2.5 Western Blotting

190 To confirm that candidate effector proteins had been produced in *N. benthamiana* and *N. tabacum*  
191 leaves using ATTAs, and to determine whether these proteins were of the predicted size, Western  
192 blotting was conducted with total protein as described previously by Guo et al. (2020). For protein  
193 separation by SDS-PAGE, 12% separating and 5% stacking gels were used, with proteins transferred  
194 to PVDF membranes. Anti-FLAG® M2 primary antibody produced in mouse (Sigma-Aldrich),  
195 together with anti-mouse secondary antibody produced in chicken (Santa Cruz Biotechnology,  
196 Dallas, TX, USA) and SuperSignal® West Dura Extended Duration substrate (Thermo Fisher  
197 Scientific, Waltham, MA, USA), were used for protein detection. Proteins were visualized using an  
198 Azure Biosystems c600 Bioanalytical Imaging system (Azure Biosystems, Dublin, CA, USA).

## 199 2.6 Protein Expression and Purification

200 Genes encoding candidate effector proteins were amplified by PCR as above from the previously  
201 generated ATTA expression vectors, without their native signal peptide sequences. Here, the 5' PCR  
202 primers incorporated a FLAG-tag for detection by Western blotting. PCR primers are shown in  
203 Supplementary Table S2. PCR amplicons were gel-extracted as above and ligated, using DNA ligase  
204 (New England Biolabs), into the SmaI/EcoRI restriction sites of the expression vector pPic9-His<sub>6</sub>  
205 (Invitrogen, Carlsberg, CA, USA), which encodes an α-factor signal peptide for protein secretion and  
206 a hexa-histidine (6×His) tag for protein purification. The ligated products were then transformed into  
207 *E. coli*. The expression constructs were sequenced and contained the predicted mature sequence of  
208 the candidate effectors fused to a 6×His tag at their N-terminus. The expression cassette was  
209 linearized with SacI or SalI (New England Biolabs) restriction enzymes and transformed into *P.*  
210 *pastoris* GS115, according to Kombrink (2012).

211 Protein expression in *P. pastoris* was performed according to Weidner et al. (2010). Briefly, protein  
212 expression was induced in 200 mL of BMMY (Buffered Methanol-complex Medium), through the

213 addition of methanol to a concentration of 0.5% (v/v) every 24 h, for 72 h. The cells were then  
214 removed by centrifugation at 4,500 g for 30 min and the supernatant filter-sterilized by passage  
215 through a 0.22 µm membrane (ReliaPrep, Ahlstrom, Helsinki, Finland). Finally, the pH of the  
216 sterilized culture filtrate was adjusted to 8 with NaOH.

217 The secreted candidate effector protein (fused with an N-terminal 6×His tag) was purified from  
218 culture filtrate using immobilized metal ion affinity chromatography (IMAC), in conjunction with a  
219 Ni Sepharose™ 6 Fast Flow (GE Healthcare, Chicago, IL, USA) column, according to the  
220 manufacturer's protocol. Before loading, the column (Glass Econo-Column® - BioRad, Hercules,  
221 CA, USA) was packed with 5 mL of resin and equilibrated by washing with binding buffer (20 mM  
222 sodium phosphate, 0.5 M NaCl, pH 7.4). The culture filtrate was added to the column at a flow rate  
223 of 1 mL/min, and protein eluted with an elution buffer (20 mM sodium phosphate, 0.5 M NaCl and  
224 500 mM imidazole, pH 7.4). The elution fractions were mixed, and elution buffer was added to a  
225 final volume of 50 mL to obtain sufficient volume for vacuum-infiltration of pine shoots. Western  
226 blotting was performed as above to determine the presence of each candidate effector protein in *P.*  
227 *pastoris* culture filtrate and after purification. Protein concentrations in culture filtrates and purified  
228 solutions were determined by using a Pierce™ Coomassie (Bradford) Protein Assay Kit (Thermo  
229 Fisher Scientific), as per the manufacturer's protocol.

## 230 **2.7 Pine Infiltration with Purified Proteins**

231 Proteins were infiltrated into tissue-cultured pine shoots at a concentration of approx. 20 µg/mL  
232 using the method developed by Hunziker et al. (2021). Briefly, clonal rootless pine shoots were  
233 maintained in LPch agar (Hargreaves et al., 2004) in glass jars, with each jar containing 6–8 shoots.  
234 For this experiment, clonal shoots originating from two relatively *Dothistroma*-susceptible families  
235 (S6 and S11) and one relatively *Dothistroma*-tolerant family (R4) (based on comparative field data)  
236 were used. The shoots were completely submerged in approx. 50 mL of each purified candidate  
237 protein or control solution (positive control: DsEcp32-3; negative control: elution buffer). Samples  
238 were exposed to vacuum in a glass chamber for 5 min to facilitate protein uptake. Shoots were then  
239 briefly rinsed in sterile MilliQ (MQ) water and subsequently placed back into the LPch agar in the  
240 glass jar. The experiment was conducted at 22°C in a room with natural light. Photos were taken 7  
241 days after infiltration (dai) using a Nikon D7000 camera.

## 242 **2.8 Tobacco Rattle Virus (TRV)-mediated Virus-induced Gene Silencing (VIGS)**

243 Fragments used to generate virus-induced gene silencing (VIGS) constructs were amplified by PCR  
244 from cDNA or genomic DNA of *N. benthamiana* using PrimeSTAR GXL DNA Polymerase (Takara  
245 Bio Inc.) with the primers listed in Supplementary Table S2. The TRV VIGS system is composed of  
246 pTRV-RNA1, which encodes replication related proteins, and pTRV-RNA2, which harbors the viral  
247 coat protein, and the candidate fragment sequences that target silencing to the corresponding genes  
248 (Liu et al., 2002; MacFarlane, 1999). The purified fragments were cloned into the pTRV-RNA2  
249 vector (Dong et al., 2007) using the ClonExpress II One Step Cloning Kit (Vazyme Biotech Co., Ltd,  
250 Nanjing, China). The resulting vectors were verified by sequencing and individually transformed into  
251 *A. tumefaciens* strain. DsEcp20-3 was screened against around 100 TRV VIGS constructs which  
252 targeted different *N. benthamiana* LRR-RLP and LRR-RLK-encoding genes. Information on this  
253 library of silencing constructs can be found in Supplementary Data 1 from Wang et al. (2018).  
254 Primers for *T26*, *T26-2*, TRV:BAK1 (Heese et al., 2007) and TRV:SOBIR1 (Liebrand et al., 2013) are  
255 shown in Supplementary Table S2.

256 *A. tumefaciens* strains carrying *N. benthamiana* gene silencing vectors (Wang et al., 2018) were  
257 grown overnight in LB medium with the appropriate antibiotics. *A. tumefaciens* cells were pelleted as  
258 mentioned above, resuspended, and incubated in infiltration medium (10 mM 2-[N-morpholino]  
259 ethanesulfonic acid pH 5.6, 10 mM MgCl<sub>2</sub>, 200 μM acetosyringone) for 3–4 h before  
260 agroinfiltration. *A. tumefaciens* cultures expressing pTRV-RNA2 constructs were mixed in a 1:1 ratio  
261 with *A. tumefaciens* culture expressing pTRV1 to a final OD<sub>600</sub> of 1.0 before infiltration into  
262 cotyledons of four-leaf-stage *N. benthamiana* seedlings. *P. sojae* NPP1 and XEG1 (Fellbrich et al.,  
263 2002; Ma et al., 2015), and *P. infestans* INF1 were used as cell death-eliciting controls for VIGS.  
264 XEG1- and INF1-triggered cell death was known to be compromised in *N. benthamiana* leaves  
265 treated with TRV:BAK1 or TRV:SOBIR1, but not with TRV:GFP, which was used as a negative  
266 control. (Wang et al., 2018).

## 267 2.9 RNA Isolation and Quantitative Reverse Transcription PCR

268 To determine the expression levels of *BAK1*, *SOBIR1* and *T26* in the TRV-mediated VIGS  
269 experiment, *N. benthamiana* leaves of similar size were selected and ground to a powder in liquid  
270 nitrogen. Total RNA was isolated from 100 mg of ground material using the E.Z.N.A.® Total RNA  
271 Kit I (Omega Bio-tek) and used as a template for first strand cDNA synthesis with PrimeScript  
272 Reverse Transcriptase (Takara Bio Inc., Kusatsu, Shiga, Japan). Quantitative reverse transcription  
273 PCR (qRT-PCR) was performed on an ABI 7500 Fast Real-Time PCR system (Applied Biosystems  
274 Inc., Foster City, CA, USA) using PrimeScript RT Master Mix (Takara Bio Inc.) with translation  
275 elongation factor 1 alpha (*EF-1α*) as an endogenous control and the primers listed in Supplementary  
276 Table S2. Data were analyzed using the 2<sup>-ΔΔCT</sup> method (Livak & Schmittgen, 2001).

## 277 3 Results

### 278 3.1 Two *D. septosporum* Elicitors are Effector Candidates that Form Part of Protein Families 279 with Orthologs in *F. fulva*

280 In our previous work, two small, secreted candidate effector proteins from *D. septosporum* NZE10,  
281 Ds70694 and Ds70057, triggered cell death in the non-host species *N. tabacum* and *N. benthamiana*  
282 (Hunziker et al., 2021). Both proteins are homologs of Ecps from *F. fulva* and are part of two  
283 different protein families, Ecp20 and Ecp32, respectively (Mesarich et al., 2018). More specifically,  
284 Ds70694 is an ortholog of FfEcp20-3 from *F. fulva* and was therefore named DsEcp20-3, whilst  
285 Ds70057 is an ortholog of FfEcp32-3 and was therefore named DsEcp32-3.

286 The Ecp20 family has four paralogues in both species. Based on sequence similarities between them,  
287 DsEcp20-3 and FfEcp20-3, together with the other orthologous pairs Ds/FfEcp20-1, Ds/FfEcp20-2  
288 and Ds/FfEcp20-4, were grouped together (Figure 1A, Supplementary Figure S1A). Interspecies  
289 pairwise amino acid identities between all family members from *D. septosporum* and *F. fulva* ranged  
290 from 10.6% to 85.5%, while intraspecies pairwise identities between all family members ranged from  
291 14.2% to 40.9% in *D. septosporum* and 11.8% to 44.2% in *F. fulva* (Supplementary Table S3). The  
292 *Ds/FfEcp20-1* genes contain one exon, with the intron located at the same position, while genes  
293 *Ds/FfEcp20-2*, -3 and -4 do not have any introns (Supplementary Figure 2A). All genes encode a  
294 protein with four cysteine residues, although the location of these varies slightly from protein pair to  
295 protein pair (Supplementary Figures S1A and S2A).

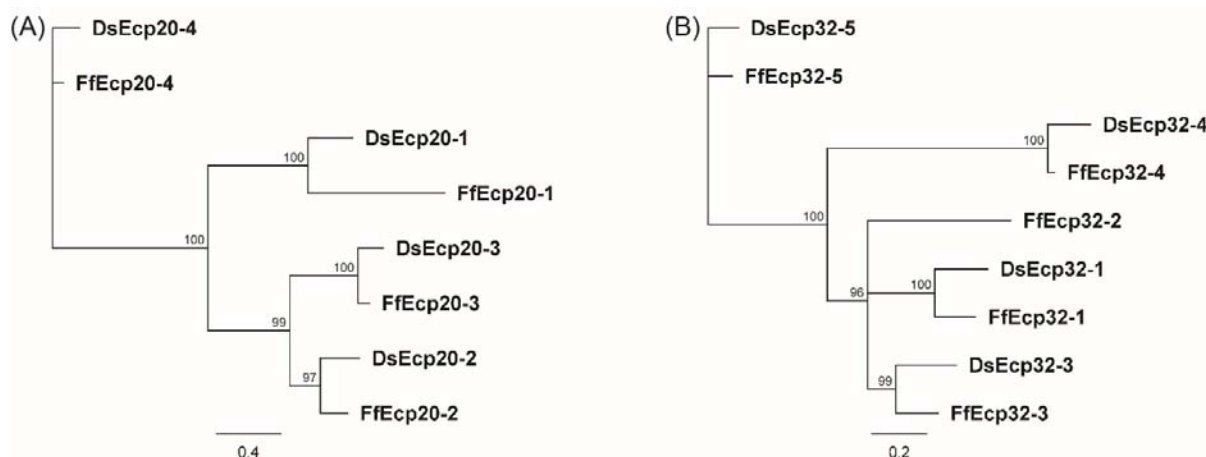
296 Based on data from a previously published transcriptome study (Bradshaw et al., 2016), all genes of  
297 the *D. septosporum* Ecp20 family are expressed during pine infection, with *DsEcp20-3* and *DsEcp20-4*  
298 being the two most highly expressed (Supplementary Table S4). *DsEcp20-3* showed strong up-

299 regulation in the Mid and Late *in planta* stages that mark the start and end of necrotrophic infection,  
300 when compared with the Early (biotrophic) stage and *in vitro*, while *DsEcp20-4* is strongly up-  
301 regulated in the Late *in planta* stage. For the corresponding genes in *F. fulva* during tomato infection,  
302 as based on data from a previously published transcriptome study (Mesarich et al., 2018), *FfEcp20-2*  
303 and *FfEcp20-3* were highly expressed throughout the timepoints analyzed, while *FfEcp20-4* was  
304 highly expressed at the beginning of infection and downregulated at later time points, when  
305 compared with *in vitro* (Supplementary Table S4). It should be noted that *FfEcp20-1* had no gene  
306 model and therefore had no FPKM value assigned to it in the previous study (Mesarich et al., 2018).  
307 Thus, no expression information was available for this gene.

308 The *Ds/FfEcp32* family was analyzed in the same way as the *Ds/FfEcp20* family above. The *Ecp32*  
309 family has five paralogues in *F. fulva*, named *FfEcp32-1* to -5, and four in *D. septosporum*, named  
310 *DsEcp32-1* and *DsEcp32-3* to -5 (there is no ortholog of *FfEcp32-2* in *D. septosporum*) (Figure 1B,  
311 Supplementary Figure S1B). Interspecies pairwise amino acid identity between all family members  
312 from *D. septosporum* and *F. fulva* ranged from 10.6% to 82%, while intraspecies pairwise identity  
313 between members ranged from 22.1% to 42.1% in *D. septosporum* and 21.6% to 49% in *C. fulvum*  
314 (Supplementary Table S3). Regarding the exon-intron structure, *Ds/FfEcp32-1*, *FfEcp32-2* and  
315 *Ds/FfEcp32-3* do not have any introns. In contrast, the *Ds/FfEcp32-4* gene pair has one intron at the  
316 same position, while the *Ds/FfEcp32-5* gene pair has two introns at the same positions  
317 (Supplementary Figure S2B). In terms of cysteine residues, the *Ds/FfEcp32* proteins have anywhere  
318 from none (*Ds/FfEcp32-5*) to five (*Ds/FfEcp32-4*), although in the case of *DsEcp32-3*, an additional  
319 cysteine is present compared to the *Ff* ortholog (Supplementary Figures S1B and S2B).

320 All *DsEcp32* genes are also expressed during pine infection. However, only *DsEcp32-3* and  
321 *DsEcp32-5* are highly expressed *in planta*, especially at the Mid and Late necrotrophic stages when  
322 compared with *in vitro*. *DsEcp32-1* and *DsEcp32-4* are only expressed at a low level *in planta*.  
323 During *F. fulva* infection of tomato, *FfEcp32-1*, *FfEcp32-2* and *FfEcp32-3* are highly expressed at all  
324 timepoints. *FfEcp32-4* was not expressed under any condition, while *FfEcp32-5* was only expressed  
325 at 12 dpi, and was downregulated compared with *in vitro* (Supplementary Table S4).

326 Genomes from the two species are mesosyntenic (de Wit et al., 2012; Zaccaron et al., 2022) and, in  
327 keeping with this, we found conservation of chromosome location between the two species for each  
328 of the *Ds/FfEcp20* and *Ds/FfEcp32* gene pairs (Supplementary Figure S3). Taken together, sequence  
329 similarity, intron position and chromosome localization suggest a common evolutionary origin for the  
330 *Ecp20* and *Ecp32* genes from both species.

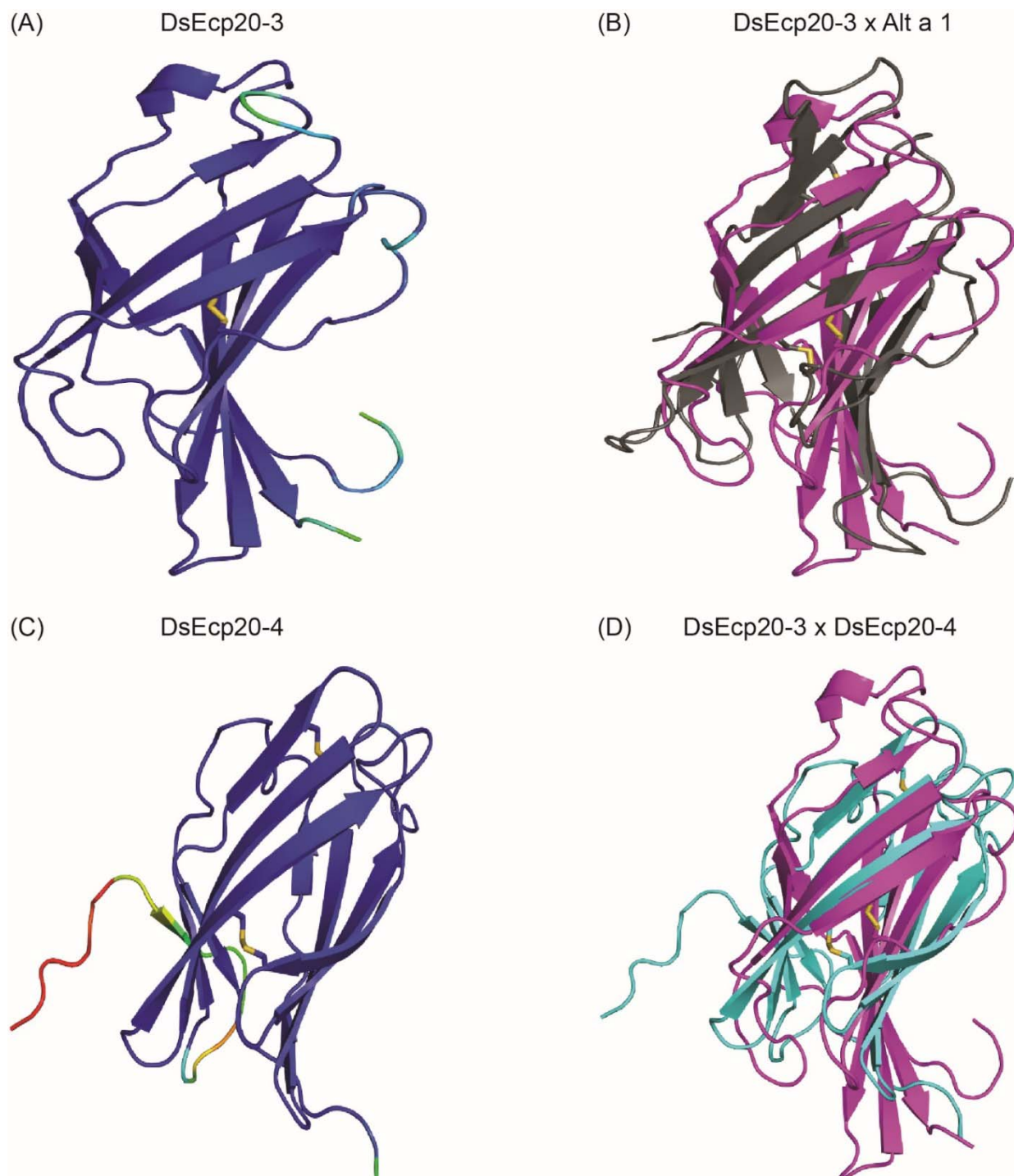


332 **Figure 1.** Protein phylogenies of the *Dothistroma septosporum* and *Fulvia fulva* Ecp20 (A) and  
333 Ecp32 (B) families. The trees were constructed with the neighbor-joining method using Geneious  
334 Software v9.1.8. Bootstrap values are shown at the nodes as percentages. The scale bar represents 0.4  
335 (A) and 0.2 (B) substitutions per site. Ds: *D. septosporum*; Ff: *F. fulva*.

336 **3.2 Predicted Tertiary Structures of Ecp20 and Ecp32 Family Members Suggest Possible  
337 Roles in Virulence**

338 We predicted the tertiary structures of all Ecp20 family members from *D. septosporum* NZE10 and  
339 *F. fulva* 0WU using AlphaFold2 (Figure 2; Supplementary Figure S4). All proteins from the Ecp20  
340 family are predicted to be structurally similar to the characterized  $\beta$ -barrel fold of Alt a 1 from  
341 *Alternaria alternata* (RCSB protein data bank [PBD] ID: 3V0R) (Chruszcz et al., 2012)  
342 (Supplementary Table S4 and S5). Figure 2 shows the predicted structures for DsEcp20-3 and  
343 DsEcp20-4, as well as the alignments between DsEcp20-3 and the characterized structure of Alt a 1  
344 from *A. alternata* and between the predicted structures of DsEcp20-3 and DsEcp20-4. The predicted  
345 structures for all the DsEcp20 and FfEcp20 proteins are shown in Supplementary Figure S4 along  
346 with characterized crystal structures of similar proteins from other fungal species.

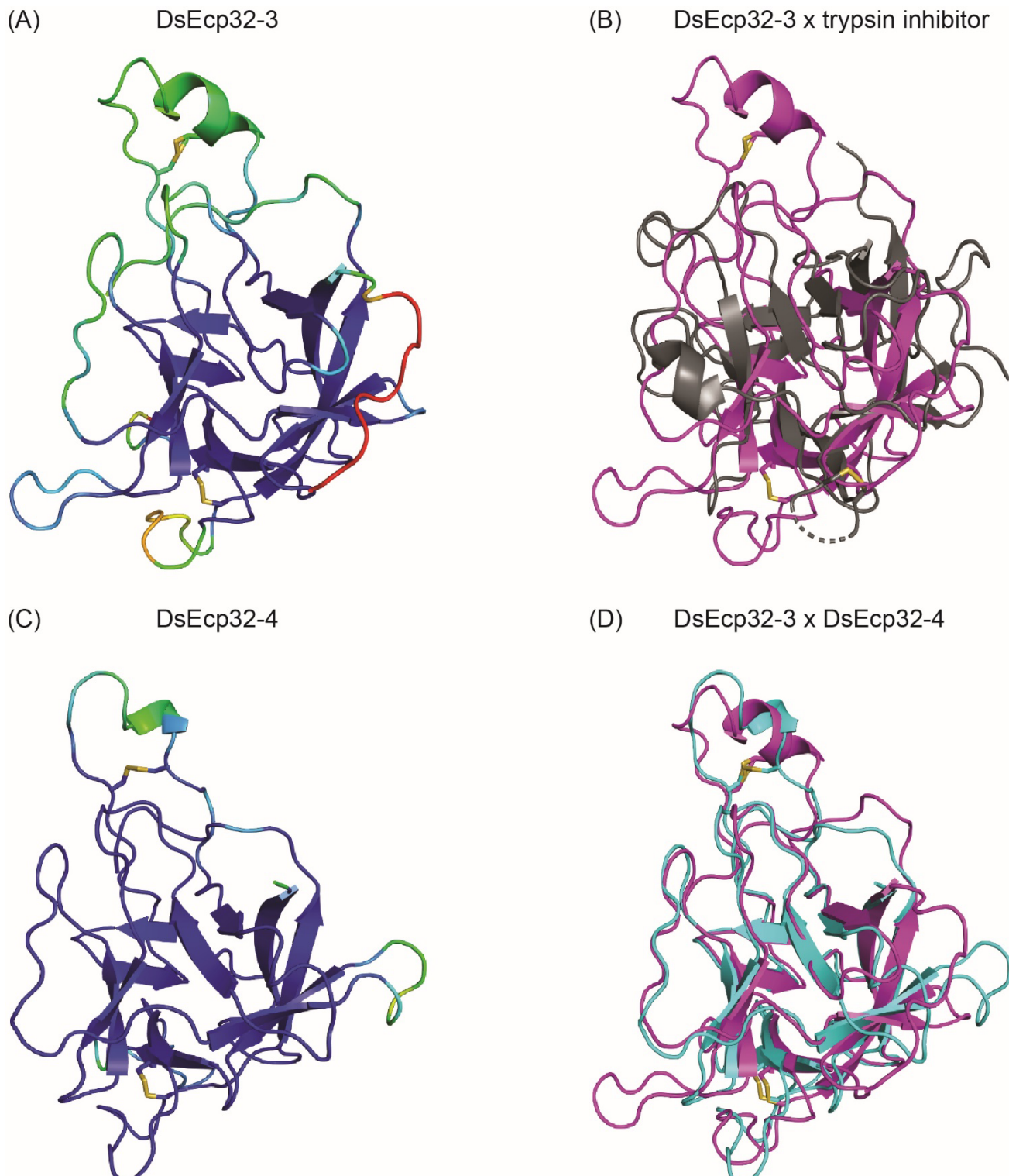
347 The tertiary structure of Ecp32 proteins was also predicted using AlphaFold2 (Figure 3,  
348 Supplementary Figure S5). All Ecp32 family members had significant hits with trypsin inhibitors and  
349 lectins; these are proteins that share a  $\beta$ -trefoil fold and are known virulence factors in plant-  
350 pathogenic fungi (Renko et al., 2012; Sabotič et al., 2019; Varrot et al., 2013) (Supplementary Table  
351 S5). Figure 3 shows the predicted structures for DsEcp32-3 and DsEcp32-4, as well as the alignments  
352 between DsEcp32-3 and the characterized structure of a trypsin inhibitor from the plant species  
353 *Enterolobium contortisiliquum* (RCSB PBD ID: 4J2K) (Zhou et al., 2013), which is the top hit in the  
354 PDB for most Ds/FfEcp32 proteins. The alignment between the predicted structures of DsEcp32-3  
355 and DsEcp32-4 is also shown in Figure 3, while all the predicted Ds/FfEcp32 structures can be found  
356 in Supplementary Figure S5 along with characterized structures of similar proteins.



357

358 **Figure 2.** Predicted protein tertiary structures of Ecp20 family members from *Dothistroma*  
359 *septosporum*. (A) Predicted structure of DsEcp20-3. (B) Alignment of the predicted DsEcp20-3  
360 structure (pink) with the characterized structure of Alt a 1 (black) from *Alternaria alternata* (RCSB  
361 protein data bank [PBD] ID: 3V0R) (Chruszcz et al., 2012). (C) Predicted structure of DsEcp20-4.  
362 (D) Alignment of predicted DsEcp20-3 (pink) and DsEcp20-4 (blue) structures. Disulphide bonds are  
363 shown as yellow sticks. Protein structures were predicted with AlphaFold2, rendered in PyMol v2.5  
364 and aligned using the CEalign tool (DeLano, 2002; Jumper et al., 2021; Mirdita et al., 2022).  
365 Structures on the left were colored in PyMol according to their AlphaFold2 pLDDT score: dark blue

366 for regions predicted with high confidence, light blue and green for regions of low confidence, and  
367 red for very low confidence regions.



368

369 **Figure 3.** Predicted protein tertiary structure of Ecp32 family members from *Dothistroma*  
370 *septosporum*. (A) Predicted structure of DsEcp32-3. (B) Alignment of the predicted DsEcp32-3  
371 (pink) structure with the characterized structure of trypsin inhibitor (black) from *Enterolobium*

372 *contortisiliquum* (RCSB protein data bank [PBD] ID: 4J2K) (Zhou et al., 2013). (C) Predicted  
373 structure of DsEcp32-4. (D) Alignment of predicted DsEcp32-3 (pink) and DsEcp32-4 (blue)  
374 structures. Disulphide bonds are shown as yellow sticks. Protein structures were predicted with  
375 AlphaFold2, rendered in PyMol v2.5 and aligned using the CEalign tool (DeLano, 2002; Jumper et  
376 al., 2021; Mirdita et al., 2022). Structures on the left were colored in PyMol according to their  
377 AlphaFold2 pLDDT score: dark blue for regions predicted with high confidence, light blue and green  
378 for regions of low confidence, and red for very low confidence regions.

379 **3.3 Ecp20 and Ecp32 Family Members are Conserved Across Other Fungal Species and *D.***  
380 ***septosporum* isolates**

381 The Ecp20 family is present in fungal species from other classes. DsEcp20-1 had 27 significant  
382 BLASTp hits in the JGI MycoCosm protein database. Two of these were from other Dothideomycete  
383 species (including the ortholog in *F. fulva*), while the rest were with species in the  
384 Eurotiomycetes class (Supplementary Table S6). DsEcp20-2 and DsEcp20-3, the most closely related  
385 to each other among the DsEcp20 family members (Figure 1A), both had the same 28 hits in JGI. All  
386 of these matches were with other Dothideomycete species and, of these, 24 were hits to proteins from  
387 other plant pathogens (Supplementary Table S6). DsEcp20-4 had 1,006 hits in the JGI MycoCosm  
388 protein database, of which 241 were proteins from plant pathogens (Supplementary Table S6).

389 In general, the Ecp32 family is more widely conserved among other fungal species compared to the  
390 Ecp20 family. Individual searches in the JGI MycoCosm protein database for each of the DsEcp32  
391 family members yielded approximately 1,000 hits for each family member (Supplementary Table  
392 S6). Those hits included proteins from fungal species with different lifestyles, ranging from  
393 saprophytes, to biotrophs, hemibiotrophs and necrotrophs. For example, DsEcp32-3 had 158 hits to  
394 proteins from fungal plant pathogens in JGI. Of these, 42 were with other members from the  
395 Mycosphaerellaceae family. These included *Cercospora zeae-maydis* with four paralogs,  
396 *Pseudocercospora (Mycosphaerella) eumusae* with six, *Pseudocercospora fijiensis* with five and  
397 *Zymoseptoria tritici* with three paralogs (Supplementary Table S6).

398 *Dothistroma pini* is also a causal agent of DNB (Barnes et al., 2004). Thus, we searched for orthologs  
399 of DsEcp20/32 encoded in the *D. pini* genome. All proteins from the *D. septosporum* Ecp20 and  
400 Ecp32 families had orthologs in the genome of *D. pini*, except Ecp32-5, for which the gene encoding  
401 this protein appears to be a pseudogene. The protein sequences were very similar between family  
402 members from the two *Dothistroma* species, with full-length pairwise amino acid identity varying  
403 from 81.1% to 93.8% (Supplementary Tables S1 and S3).

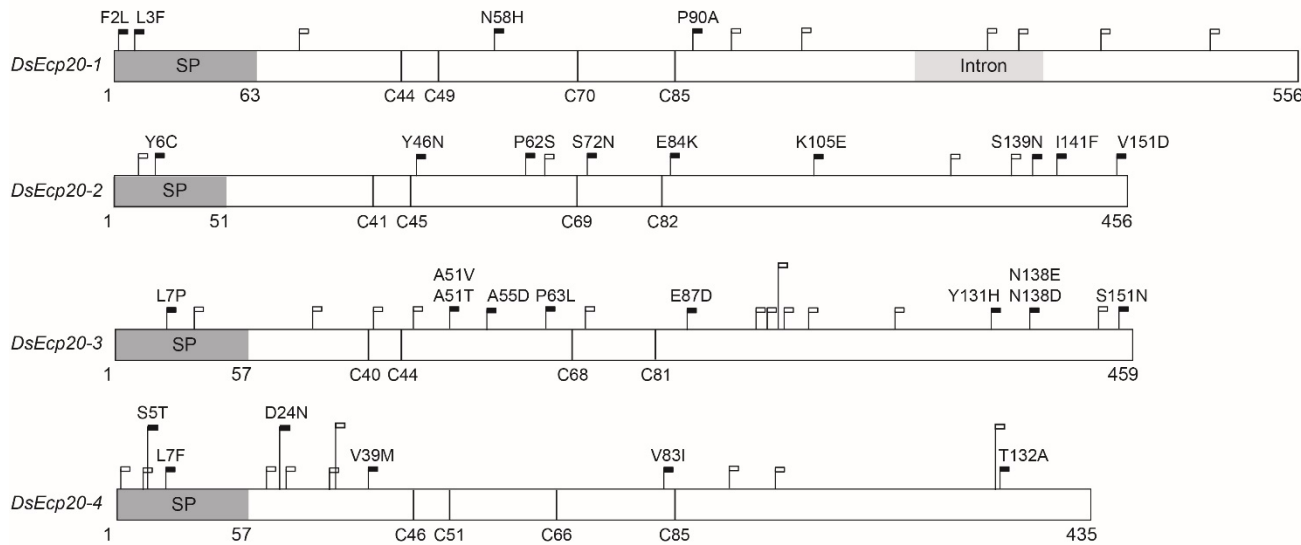
404 We next addressed the question of whether the *D. septosporum* Ecp20 and Ecp32 family genes are  
405 conserved in other isolates of this species and whether they are identical in sequence to NZE10.  
406 Genome sequences were available from 18 *D. septosporum* isolates collected from different  
407 geographic locations (Bradshaw et al., 2019). All members of the *D. septosporum* Ecp20 and Ecp32  
408 families were present in the 18 other genomes. In each of these genomes, there was at least one single  
409 nucleotide polymorphism (SNP) leading to an amino acid difference in at least one family member  
410 for both Ecp20 and Ecp32 (Supplementary Table S7).

411 A total of 59 different SNPs were identified among the Ecp20 family members across the 18 *D.*  
412 *septosporum* isolates, compared to NZE10 (Figure 4). DsEcp20-1, DsEcp20-2 and DsEcp20-4 had  
413 approximately the same number of SNPs: 11, 13 and 15, respectively, while DsEcp20-3 had a total of  
414 20. For DsEcp20-1, DsEcp20-3 and DsEcp20-4, however, most SNPs (61%, 60% and 60%,  
415 respectively) were synonymous. In the case of DsEcp20-2, however, only 30% were synonymous

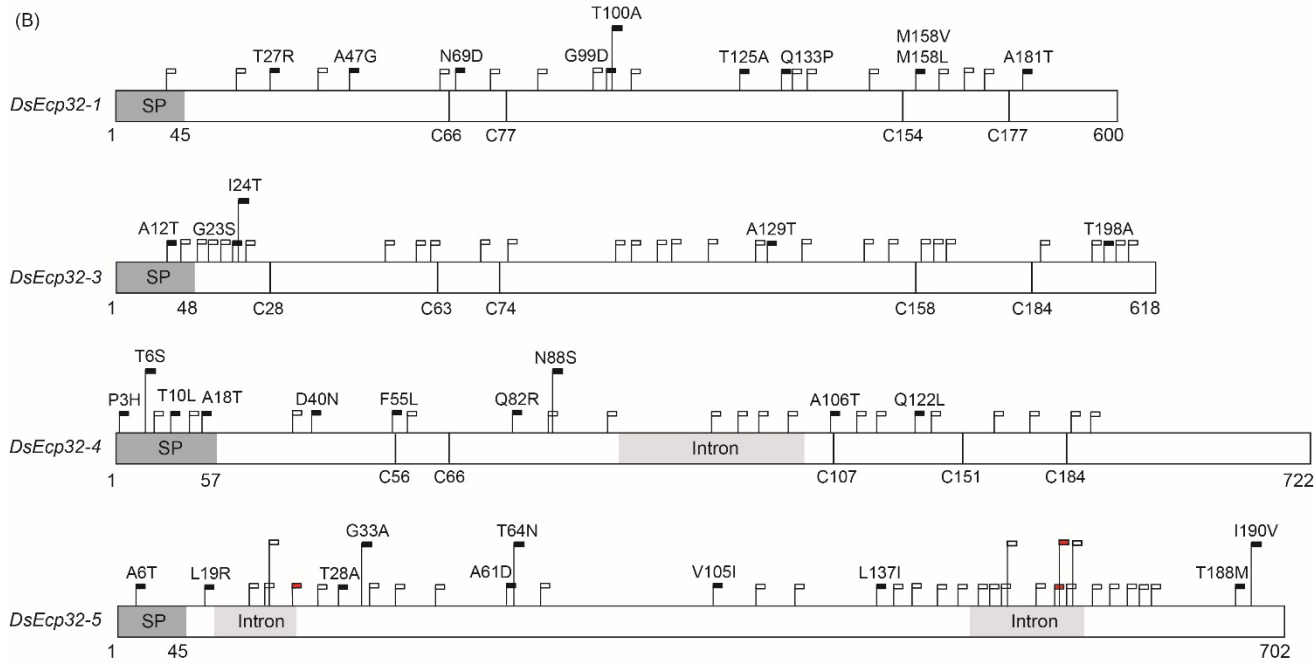
416 and a higher number of SNPs leading to an amino acid difference (9 out of 13; 70%) were observed  
417 (Figure 4A). The *Ecp32* gene family had a higher number of DNA modifications across the 18 *D.*  
418 *septosporum* genomes analyzed, with a total of 117 SNPs and 3 insertions. The two most  
419 polymorphic genes were *DsEcp32-3* and *DsEcp32-5*. Interestingly, while *DsEcp32-3* had 31  
420 sequence modifications, only five of these led to an amino acid difference (16%). All other family  
421 members had 9 or 10 SNPs leading to an amino acid difference (Figure 4B).

422 The Guatemalan (GUA1 and GUA2) and Colombian (COLN and COLS) isolates showed the greatest  
423 amino acid sequence diversity, when compared to strain NZE10, for both the *Ecp20* and *Ecp32*  
424 family members. For *DsEcp20-1*, the most diverse isolates were COLN and COLS, with identical  
425 sequences, while COLN had the most sequence variation in *DsEcp32-1*. For *DsEcp20-2* and -4, and  
426 *Ecp32-3*, -4, and -5, both Guatemalan isolates were the most diverse and, for *DsEcp20-3*, GUA2 had  
427 greater amino acid diversity (Supplementary Table S7).

(A)



(B)



428

429 **Figure 4.** Schematic diagram showing sequence variation in *Dothistroma septosporum* NZE10  
430 Ecp20 (A) and Ecp32 (B) family members across 18 other *D. septosporum* isolates. Dark grey boxes  
431 indicate signal peptide positions and light grey boxes indicate intron positions. Black flags show the  
432 position of nucleotide variations that led to non-synonymous changes, with the specific amino acid  
433 differences indicated above the flags. White flags show the position of synonymous nucleotide  
434 variations. Red flags show the position of nucleotide insertions. Vertical black lines show the  
435 positions of cysteine residues. Nucleotide positions are shown under each gene. SP: signal peptide.

436 **3.4 Other Members of the Ecp20 and Ecp32 Families from *D. septosporum* and *F. fulva***  
437 **Trigger Cell Death Responses in Non-host Plants**

438 Following on from a previous study in which DsEcp20-3 and DsEcp32-3 were shown to elicit cell  
439 death in the non-host plants *N. benthamiana* and *N. tabacum* using ATTAs (Hunziker et al., 2021),

440 we set out to determine whether other family members of both *D. septosporum* and *F. fulva* could  
441 elicit the same response. To achieve this, all Ecp20 and Ecp32 family members were transiently  
442 expressed in *N. benthamiana* and *N. tabacum* using ATTAs, and the percentages of plant responses  
443 in three different categories recorded: strong cell death, weak cell death and no cell death (Figure 5;  
444 Supplementary Figure S6). Here, orthologous pairs from both pathogens were tested on the same  
445 leaf, so that differences between them could be better assessed.

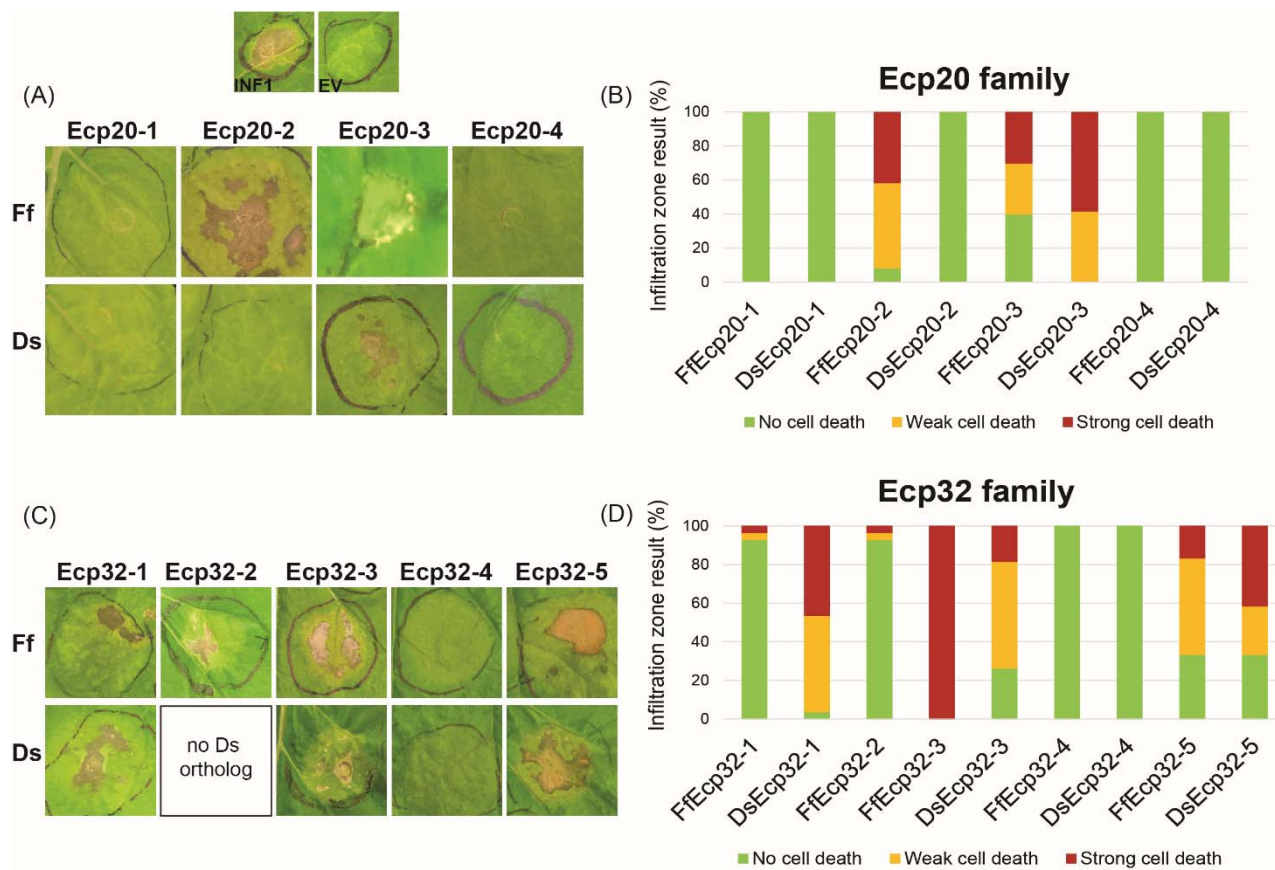
446 As expected, the positive control INF1 triggered strong cell death responses and the negative control  
447 empty vector did not elicit a response. Among Ecp20 family members, FfEcp20-2 triggered strong or  
448 weak cell death responses in *N. benthamiana* in 91.7% of infiltration zones, whilst its ortholog  
449 DsEcp20-2 did not elicit any cell death responses. Both FfEcp20-3 and DsEcp20-3 caused consistent  
450 plant cell death in *N. benthamiana*, with DsEcp20-3 having 58% of infiltration zones showing strong  
451 cell death across the entire infiltration zone (Figure 5A, 5B). In *N. tabacum*, DsEcp20-3 was the only  
452 family member that triggered a cell death response (Supplementary Figure S6). Interestingly,  
453 DsEcp20-4, one of the most highly expressed secreted proteins during infection of pine by *D.*  
454 *septosporum* (Supplementary Table S4; Bradshaw et al. (2016)), and its ortholog from *F. fulva*,  
455 FfEcp20-4, did not induce cell death responses in either *N. benthamiana* or *N. tabacum* (Figure 5;  
456 Supplementary Figure S6).

457 The ability of Ecp32 family members to trigger cell death was also assessed in both *Nicotiana*  
458 species. In this case, all proteins from the Ecp32 family, apart from the Ds/FfEcp32-4 protein pair,  
459 induced some degree of cell death in both plant species. Interestingly, DsEcp32-1 consistently  
460 triggered cell death in *N. benthamiana*, while its ortholog from *F. fulva*, FfEcp32-1, only caused a  
461 strong cell death response in 3.5% of infiltration zones across all replicates (Figure 5C, 5D). In  
462 contrast, in *N. benthamiana*, FfEcp32-3 was capable of triggering consistent strong cell death  
463 responses, while DsEcp32-3 only triggered a strong response in approximately 20% of infiltration  
464 zones. The Ds/FfEcp32-5 pair triggered similar degrees of cell death responses in *N. benthamiana*  
465 (Figure 5D).

466 To determine whether apoplastic localization is required for members of the Ecp20 and Ecp32  
467 families to trigger cell death, proteins that previously elicited a plant response, but lacked the PR1 $\alpha$   
468 signal peptide for secretion to the apoplast, were transiently expressed in *N. benthamiana*. Without  
469 the signal peptide, none of proteins tested were able to cause cell death (Supplementary Figure S7  
470 and Supplementary Figure S8).

471 In cases where a cell death response was not observed at all, or where only weak cell death was  
472 observed, a Western blot analysis was performed to confirm the presence of the proteins in the tissue  
473 of the infiltrated plants (Supplementary Figure S8). All proteins that did not trigger cell death or only  
474 triggered a weak cell death response were detected via Western blot, indicating that the lack of cell  
475 death response was not due to absence of those proteins.

476 Taken together, these results indicate that Ecp20 and Ecp32 family members from two closely related  
477 fungal pathogens, *D. septosporum* and *F. fulva*, differ in their ability to induce a cell death response  
478 in non-host species. Furthermore, the finding that proteins without a signal peptide failed to trigger a  
479 plant cell death response, suggests that secretion into the apoplastic environment of *N. benthamiana*  
480 is essential for their cell death-eliciting activity.



481

482 **Figure 5.** Ecp20 and Ecp32 proteins from *Dothistroma septosporum* NZE10 and *Fulvia fulva* 0WU  
483 trigger cell death responses in the non-host plant *Nicotiana benthamiana*. Ecp20 (A) and Ecp32 (C)  
484 family members from *D. septosporum* and *F. fulva* were expressed in *N. benthamiana* using an  
485 *Agrobacterium tumefaciens*-mediated transient expression assay (ATTA) to assess their ability to  
486 elicit cell death. Representative images are shown (n = 12–24 infiltration zones), from at least three  
487 independent experiments. INF1, *Phytophthora infestans* elicitin positive cell death control; EV,  
488 empty vector negative no cell death control; Ds: *D. septosporum*; Ff: *F. fulva*. Graphs display the  
489 percentages of infiltration zones that showed cell death in response to Ecp20 (B) and Ecp32 (D)  
490 family members from *F. fulva* and *D. septosporum*, divided into three categories: strong cell death,  
491 weak cell death and no cell death. Photos were taken 7 days after infiltration.

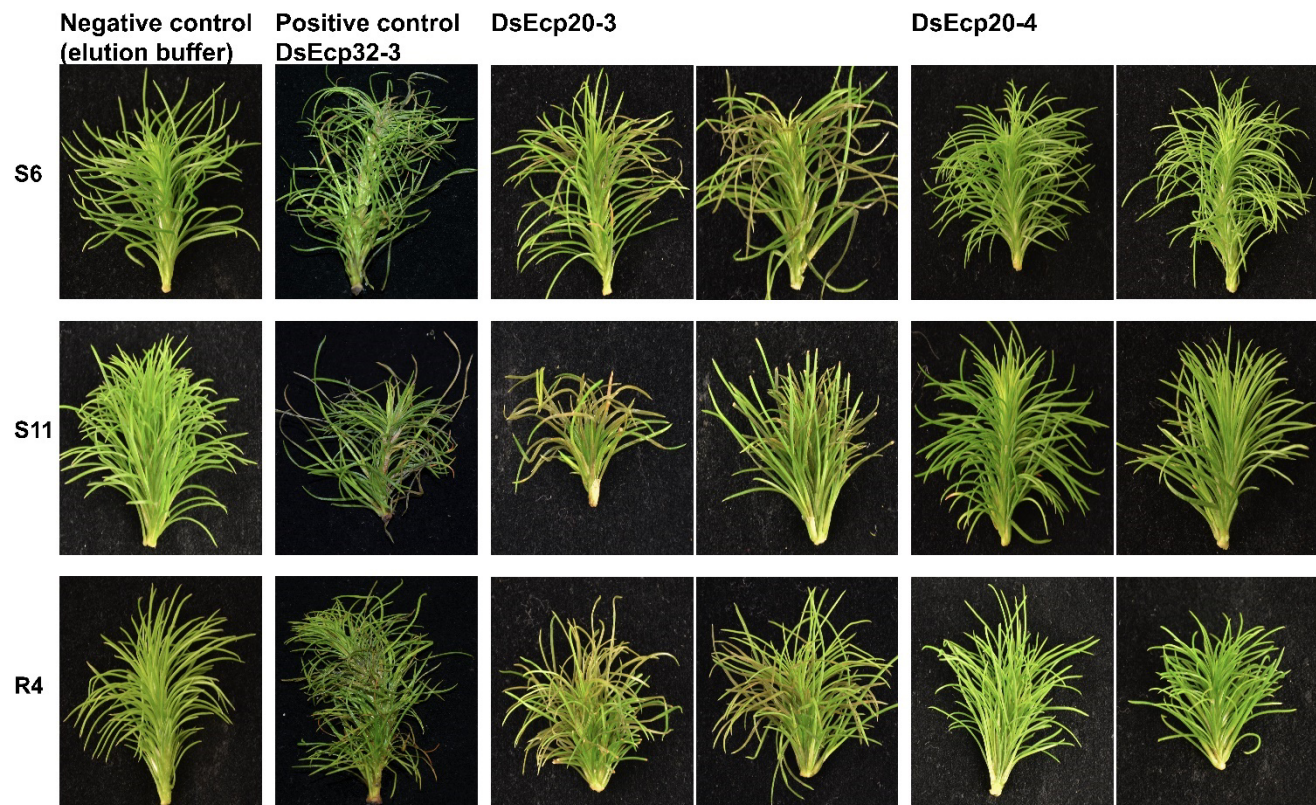
492 **3.5 Proteins from other *D. septosporum* Isolates and *D. pini* also Trigger Cell Death in Non-  
493 host Plants**

494 Alleles of some *Ecp20* and *Ecp32* family genes identified from *D. pini*, and from isolates of *D.*  
495 *septosporum* other than NZE10, were tested for the ability of their encoded proteins to trigger cell  
496 death in *N. benthamiana*. For the proteins from *D. septosporum* NZE10 that consistently triggered the  
497 highest percentages of cell death (DsEcp20-3, DsEcp32-1 and DsEcp32-3), we tested orthologs of  
498 other *D. septosporum* alleles and found they triggered the same responses as those of *D. septosporum*  
499 NZE10 (Supplementary Figure S9). The same was true for the respective orthologs of DpEcp20-3,  
500 DpEcp32-1 and DpEcp32-3 from *D. pini*, which also elicited cell death responses in *N. benthamiana*.  
501 These results suggest conservation of cell death-eliciting activity between isolates of *D. septosporum*  
502 and between the two *Dothistroma* species for members of the Ecp20 and Ecp32 families.

503 **3.6 Infiltration of Purified Ecp20 and Ecp32 Proteins from *D. septosporum* into *P. radiata***  
504 **Triggers Cell Death**

505 The pine infiltration method described in Hunziker et al. (2021) proved to be a suitable approach for  
506 testing the cell death-eliciting activity of candidate apoplastic effector proteins from pine pathogens  
507 in *P. radiata*. We previously showed that DsEcp32-3 triggered cell death in three *P. radiata*  
508 genotypes (S6, S11 and R4). Using the same method, we tested two additional proteins from the  
509 DsEcp20 family, DsEcp20-3 and DsEcp20-4, and repeated the infiltration of DsEcp32-3 as a positive  
510 cell death control (Figure 6, Supplementary Figure S10) (Hunziker et al., 2021).

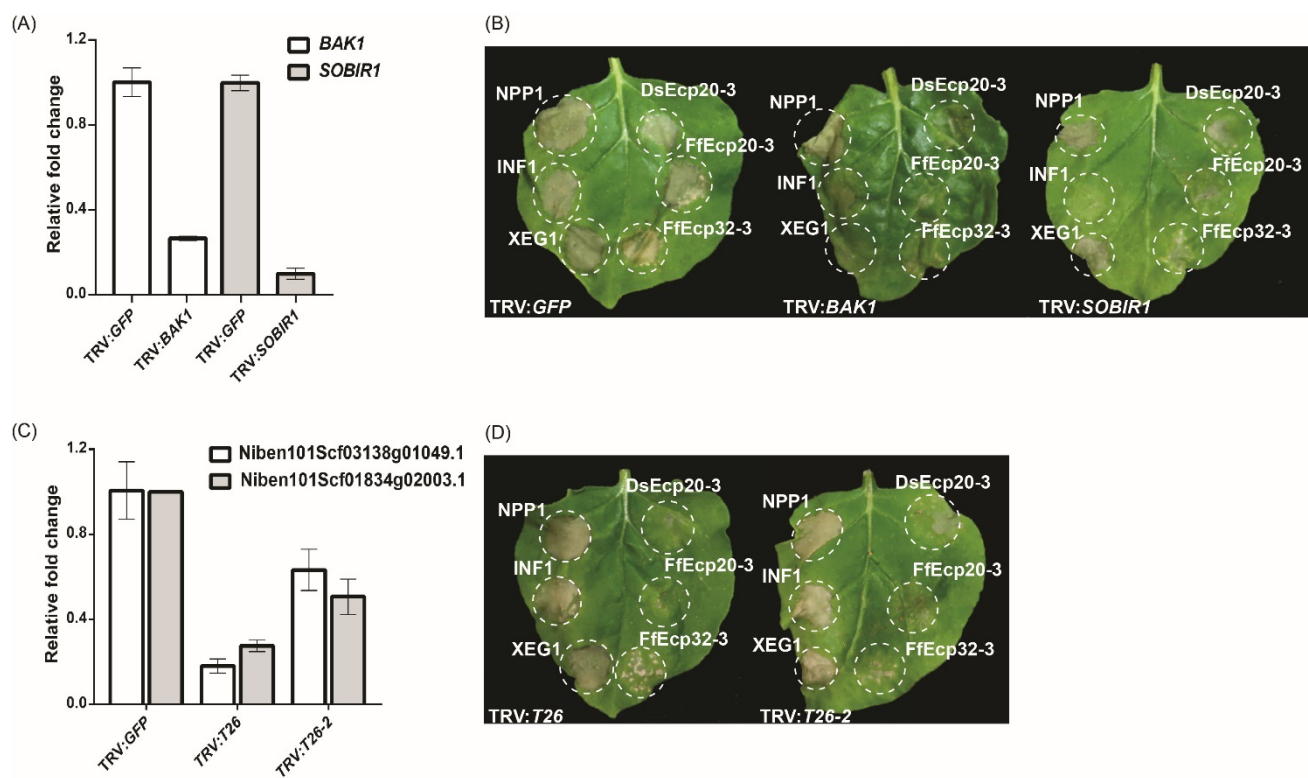
511 The DsEcp32-3 positive control triggered cell death in all three pine genotypes, as expected (Figure  
512 6). Infiltration of elution buffer (negative control) did not cause any damage or visible stress  
513 responses. Interestingly, both tested proteins gave the same response as they had shown in the non-  
514 host *Nicotiana* plants: DsEcp20-3 consistently elicited cell death in the same three pine genotypes  
515 used in the previous study, while DsEcp20-4 failed to elicit any response in the pine shoots.



517 **Figure 6.** *Dothistroma septosporum* candidate effectors DsEcp20-3 and DsEcp20-4 trigger the same  
518 responses in *Pinus radiata* shoot tissues following vacuum infiltration as in non-host plants. Whole  
519 shoots of *P. radiata* derived from family seedlots that are relatively susceptible (S6 and S11) or  
520 tolerant (R4) to *D. septosporum* infection were infiltrated with purified DsEcp20-3 and DsEcp20-4  
521 proteins produced by heterologous expression in *Pichia pastoris*. Elution buffer was used as negative  
522 control and purified DsEcp32-3 protein as a positive control. Representative photos (from 18 to 24  
523 pine shoots for each treatment) were taken 7 days after infiltration.

524 **3.7 DsEcp20-3-triggered Cell Death in *N. benthamiana* requires Membrane-localized  
525 Receptor-like Proteins**

526 To determine how cell death elicitors from the Ds/FfEcp20 and 32 family were perceived by plants,  
 527 we silenced genes encoding the extracellular receptor-like kinase co-receptor genes *BAK1* and  
 528 *SOBIR1*, as well as leucine-rich repeat (LRR) receptor-like genes, in *N. benthamiana* (Figure 7), in  
 529 conjunction with agro-infiltration, as previously described by Wang et al. (2018). As expected, agro-  
 530 infiltration of positive controls NPP1, INF1 and XEG triggered consistent strong cell death responses  
 531 in *N. benthamiana* leaves treated with TRV:GFP, while INF1- and XEG1-triggered cell death was  
 532 compromised in leaves treated with TRV:BAK1 or TRV:SOBIR1. We also consistently found that  
 533 DsEcp20-3-triggered cell death was compromised in *N. benthamiana* leaves in which the receptor-  
 534 like kinase genes *BAK1* or *SOBIR1* were silenced (Figure 7B). In addition, we found that DsEcp20-3-  
 535 triggered cell death was compromised in *N. benthamiana* leaves treated with TRV VIGS constructs  
 536 TRV:T26 and TRV:T26-2 (Wang et al., 2018) (Figure 7D). TRV:T26 and TRV:T26-2 both target the  
 537 same two *N. benthamiana* genes but in different regions of those genes. One of these target genes  
 538 encodes an LRR-type extracellular receptor-like protein (Sol Genomics Network accession number -  
 539 Niben101Scf03138g01049.1) and one an extracellular LRR (Niben101Scf01834g02009.1). We  
 540 further screened other members of the Ecp20 and Ecp32 families (FfEcp20-3, DsEcp32-3 and  
 541 FfEcp32-3), and found that cell death triggered by FfEcp20-3 and FfEcp32-3 was also significantly  
 542 compromised in *N. benthamiana* leaves treated with TRV:BAK1, TRV:SOBIR1 or either of the T26  
 543 constructs (Figure 7B and D). For DsEcp32-3-triggered cell death, we did not detect any reduction on  
 544 TRV:BAK1- or TRV:SOBIR1-silenced plants (data not shown). Taken together, these results suggest  
 545 that the cell death responses triggered by members of the Ecp20 and Ecp32 families from *D. septosporum*  
 546 and *F. fulva* in *N. benthamiana* are the result of recognition by extracellular immune  
 547 receptors, and that the transduction of defense response signals following this recognition requires  
 548 the extracellular co-receptors BAK1 and SOBIR1.



549

550 **Figure 7.** Cell death triggered by DsEcp20-3 in *Nicotiana benthamiana* is compromised in leaves  
 551 silenced for different receptor-like genes. Expression levels of (A) *BAK1* and *SOBIR1* and (C) *T26*  
 552 constructs in plants silenced for these genes, relative to their expression in plants silenced for the

553 Green Fluorescent Protein (*GFP*) gene (absent in *N. benthamiana*; normalized to 1). Genes were  
554 silenced using a Virus-Induced Gene Silencing (VIGS) method based on Tobacco Rattle Virus  
555 (TRV). (C, D) Representative leaves showing cell death induced by expression of XEG1, INF1,  
556 NPP1, DsEcp20-3, FfEcp20-3 and FfEcp32-3 in *N. benthamiana* treated with specific TRV-mediated  
557 VIGS constructs as shown. Leaves (n = 8) were photographed three days after agro-infiltration (dai).  
558 Experiments were repeated twice with similar results.

559 **4 Discussion**

560 Plant-pathogenic fungi secrete a collection of virulence factors, termed effector proteins, into their  
561 hosts to promote the infection process (Lo Presti et al., 2015; Rocafort et al., 2020). While many of  
562 these effectors appear to be singletons with no obvious sequence similarity to proteins present in the  
563 effector repertoires to which they belong, others form part of families. Indeed, in *Venturia inaequalis*,  
564 the biotrophic Dothideomycete pathogen responsible for scab disease of apple, more than half of the  
565 predicted effector repertoire is made up of protein families based on sequence similarity alone (Deng  
566 et al., 2017; Rocafort et al., 2022). Likewise, in *Ciborinia camelliae*, the necrotrophic Leotiomycete  
567 pathogen responsible for flower blight disease of camellias, approximately one tenth of the predicted  
568 secretome belongs to a single massively expanded candidate effector family (Denton-Giles et al.,  
569 2020). Notably, effector families can also be associated with avirulence. For example, in the  
570 hemibiotrophic Sordariomycete pathogen *Magnaporthe oryzae* (rice blast disease), the biotrophic  
571 Leotiomycete pathogen *Blumeria graminis* (cereal powdery mildew disease), as well as the  
572 biotrophic Pucciniomycete pathogen *Melampsora lini* (flax rust disease) and the hemibiotrophic  
573 Dothideomycete pathogen *Leptosphaeria maculans* (stem canker disease of brassica), certain  
574 avirulence effectors have been found to form part of protein families (Anderson et al., 2016;  
575 Catanzariti et al., 2006; Dodds et al., 2004; Kang et al., 1995; Khang et al., 2008; Praz et al., 2017;  
576 Spanu, 2017; Talbi et al., 2022).

577 The emergence of sequence-related effector families in fungi is often the result of duplication events  
578 from an ancestral gene or from other family members and is typically followed by sequence  
579 diversification through an accumulation of indels and synonymous/non-synonymous substitutions  
580 and/or recombination events between different family members (Denton-Giles et al., 2020;  
581 Franceschetti et al., 2017; Pendleton et al., 2014). Such sequence diversification is anticipated to have  
582 roles in, for example, the diversification of effector functions, as well as the evasion of host  
583 immunity. In some cases, this diversification can result in an almost complete loss of sequence  
584 similarity between family members, with similarity only retained at the protein tertiary structure  
585 level, as has recently been shown for several effector families of plant-pathogenic fungi using the  
586 groundbreaking *ab initio* protein structure prediction tool, AlphaFold2 (Rocafort et al., 2022; Seong  
587 & Krasileva, 2022). However, in many cases, sequence identity between family members is  
588 maintained, even across different fungal species. These cross-species effector families are of high  
589 interest, as their sequence conservation may indicate an important and/or conserved (i.e., core) role in  
590 fungal virulence (Stergiopoulos et al., 2010).

591 In this study, we identified two candidate effector protein families, Ecp20 and Ecp32, which are  
592 highly conserved at the primary sequence and tertiary structure levels between the two closely related  
593 Dothideomycete fungal pathogens, *D. septosporum* and *F. fulva*. Despite their close phylogenetic  
594 relationship, these two pathogens have very different hosts, with *D. septosporum* causing disease on  
595 pine (a gymnosperm), and *F. fulva* causing disease on tomato (an angiosperm) (Drenkhan et al.,  
596 2016; Thomma et al., 2005). An investigation of pre-existing gene expression data revealed that both  
597 protein families have members encoded by genes that are highly expressed *in planta*, while others are

598 only moderately or lowly expressed. Such a finding is consistent with what was recently observed in  
599 *V. inaequalis*, where gene family members are expressed at different levels during apple infection  
600 (Rocafort et al., 2022).

601 Both the Ecp20 and Ecp32 families were found to have members that differed in their ability to  
602 trigger cell death in the non-host species *N. benthamiana* and *N. tabacum*. The differential ability of  
603 these family members to trigger a cell death response does not appear to be restricted to proteins from  
604 *D. septosporum* and *F. fulva*. Indeed, it was recently determined that an ortholog of Ds/FfEcp20-4  
605 from the hemibiotrophic Dothideomycete pathogen *Zymoseptoria tritici* (Septoria leaf blotch disease  
606 of wheat), named Zt4 (JGI protein ID 104697), triggers cell death in *N. benthamiana* (Kettles et al.,  
607 2017). This is in contrast to Ds/FfEcp20-4, where, in our study, no cell death response was observed.  
608 Similarly, a homolog of Ecp32-1 from *Z. tritici* (JGI protein ID 105896; no reciprocal ortholog in *D.*  
609 *septosporum* or *F. fulva*) was not able to induce a cell death response in *N. benthamiana* (Kettles et  
610 al., 2017) whereas in our study, DsEcp32-1 and FfEcp32-1 consistently and infrequently triggered  
611 cell death, respectively. Of course, it remains possible that some of the family members triggered  
612 other plant responses, such as changes in host gene expression or the accumulation of reactive  
613 oxygen species (ROS), which were not measured in our assays. In any case, variation in the ability of  
614 family members to elicit plant cell death is not restricted to the Ecp20 and Ecp32 families, with  
615 variation also observed in, for example, the cell death-inducing capacity of CcSSP effector candidate  
616 family members from *C. camelliae* in camellia petals (Denton-Giles et al., 2020).

617 BLASTp searches demonstrated that, like those shown above for *Z. tritici*, homologs of the Ecp20  
618 and Ecp32 family members are present in other fungal species, with many of these species being  
619 plant pathogens. Interestingly, as observed in *D. septosporum* and *F. fulva*, these homologs were also  
620 frequently found to exist as protein families. Taken together, it is therefore likely that the Ecp20 and  
621 Ecp32 proteins are core effectors, possibly contributing to conserved virulence functions in their  
622 respective plant hosts. In addition to searching for homologs in other plant pathogens, we also  
623 screened the genomes of other *D. septosporum* isolates and of *D. pini*, the other causal species of  
624 DNB, and found that whilst Ecp20 and Ecp32 family members are polymorphic across other *D.*  
625 *septosporum* isolates, all family members are present in these isolates and also in *D. pini*, with the  
626 exception of Ecp32-5. There was also conservation of cell death-eliciting function between isolates  
627 of *D. septosporum* and between the two *Dothistroma* species, since the respective orthologs showed  
628 the same responses as those from the NZE10 strain, also triggering cell death in *N. benthamiana*.  
629 Whether the identified sequence variation contributes to virulence function of these proteins outside  
630 of cell death elicitation remains to be determined.

631 As the primary amino acid sequence of the Ecp20 and Ecp32 family members provided no insights  
632 into their potential virulence function, we predicted the tertiary structures of these proteins using the  
633 AlphaFold2 tool and compared them to proteins of characterized structure and/or function. Based on  
634 this analysis, all eight *D. septosporum* and *F. fulva* Ecp20 family members were predicted to possess  
635 structural similarity to PevD1, an effector protein with an Alt a 1 ( $\beta$ -barrel) fold from the  
636 hemibiotrophic Sordariomycete pathogen *Verticillium dahliae* (Chruszcz et al., 2012; Han et al.,  
637 2012). Interestingly, the Alt a 1 fold has also been found in MoHrip1, a plasma membrane-binding  
638 virulence factor from *M. oryzae* that is highly expressed during rice infection (Zhang et al., 2017).  
639 Just like FfEcp20-2, FfEcp20-3 and DsEcp20-3, the PevD1 and MoHrip1 proteins induce cell death  
640 responses in *Nicotiana* species (Han et al., 2012; Zhang et al., 2017), suggesting that this cell death-  
641 eliciting ability could be a conserved function of these proteins. It should be noted, however, that  
642 proteins with an Alt a 1 fold, including PevD1, have also been shown to interact with and inhibit the  
643 enzymatic activity of pathogenesis-related 5 (PR5) proteins from different host plants (Gómez-

644 Casado et al., 2014; Kumar & Mukherjee, 2020; Zhang et al., 2019). Whether the Ecp20 proteins  
645 from *D. septosporum* and *F. fulva* perform a similar role in pathogen virulence remains to be  
646 explored.

647 In contrast to members of the Ecp20 family, the Ecp32 proteins were predicted to be structurally  
648 similar to proteins from diverse organisms with a  $\beta$ -trefoil fold. Proteins with a  $\beta$ -trefoil fold have the  
649 ability to recognize different ligands, such as DNA, proteins and carbohydrates, and so can be  
650 involved in different processes and interactions between organisms (Žurga et al., 2015). Among the  
651  $\beta$ -trefoil fold proteins, the most abundant members are lectins, carbohydrate-binding proteins and  
652 hydrolase inhibitors, such as protease inhibitors (Renko et al., 2012). Lectins are proteins that  
653 specifically bind carbohydrates and, in fungi, are associated with plant-pathogen interactions, fungal  
654 growth, fruiting body development and, due to their toxicity, defense against parasitic or predatory  
655 organisms (Sharon, 2007; Varrot et al., 2013). Lectins from different mushroom species, for example,  
656 are known to be toxic to organisms such as *Caenorhabditis elegans* and *Drosophila melanogaster*  
657 (Juillot et al., 2016; Schubert et al., 2012; Wohlschlager et al., 2011). These proteins bind to the  
658 plasma membrane and, in doing so, induce cell death. Cyt toxins from *Bacillus thuringiensis*, for  
659 instance, are insecticidal proteins with a  $\beta$ -trefoil fold that are known to interact with host membrane  
660 lipids (Soberón et al., 2013). Even though the mechanism of lectin toxicity is not known, it is  
661 hypothesized that this toxicity may be the direct result of host membrane damage. Taken together,  
662 this could indicate a possible role Ecp32 proteins in triggering plant cell death, at least in part, by  
663 interacting with and disrupting the host membrane.

664 As mentioned above, protease inhibitors can also adopt a  $\beta$ -trefoil fold, and in our study, it was found  
665 that most Ds/FfEcp32 proteins had a predicted tertiary structure similar to that of a plant trypsin  
666 inhibitor. Of interest, fungal pathogens frequently target host proteases involved in plant defense by  
667 secreting effectors that serve as protease inhibitors, with well characterized examples including Pit2  
668 from the biotrophic Ustilaginomycete *Ustilago maydis* (corn smut disease) and Avr2 from *F. fulva*  
669 (Mueller et al., 2013; Tian et al., 2007; van Esse et al., 2008). While it is not yet known whether Pit2  
670 or Avr2 adopt a  $\beta$ -trefoil fold, another possible function for the Ecp32 proteins could therefore  
671 involve the inhibition of plant proteases during host colonization.

672 The fact that Ecp20 and Ecp32 family members of *D. septosporum*, *F. fulva* and *Z. tritici* are likely  
673 apoplastic (Hunziker et al., 2021; Kettles et al., 2017; Mesarich et al., 2018), and that members of  
674 both families across multiple fungal species trigger cell death in *Nicotiana* species (with this activity  
675 dependent on their secretion to the apoplast), may suggest that each family presents a conserved  
676 epitope that is recognized by an extracellular immune receptor in these non-host plants. In support of  
677 recognition by an extracellular immune receptor, silencing of the extracellular co-receptors *NbBAK1*  
678 or *NbSOBIR1* in *N. benthamiana*, which are required to transduce defense response signals following  
679 apoplastic effector recognition (Liebrand et al., 2013; Liebrand et al., 2014), compromised  
680 Ds/FfEcp20-3-dependent cell death. Notably, a compromised cell death response was also observed  
681 for FfEcp32-3, but not DsEcp32-3. One possibility here is that the expression of *NbBAK1* and/or  
682 *NbSOBIR1* was not reduced to a level sufficient for the cell death response triggered by DsEcp32-3  
683 to be compromised. Alternatively, given its predicted structural similarity to lectins, other processes  
684 outside of immune receptor recognition, such as cell membrane perturbation, could be involved in  
685 cell death elicitation by DsEcp32-3.

686 In line with the cell death response observed in the non-host species, we previously determined that  
687 DsEcp32-3 can trigger cell death in pine and suggested that this protein might be a virulence factor in  
688 the necrotrophic stage of DNB that helps to destroy needle tissue (Hunziker et al., 2021). With this in

689 mind, we decided to investigate whether two (purified) *D. septosporum* proteins from the Ecp20  
690 family could also induce a cell death response in pine. Both proteins, DsEcp20-3 and DsEcp20-4,  
691 were of interest due to their high expression in the Mid and Late (necrotrophic) stages of *D.*  
692 *septosporum* infection in *P. radiata* (Bradshaw et al., 2016). The finding that DsEcp20-3 and  
693 DsEcp20-4 triggered different cell death responses in non-host plants, *N. benthamiana* and *N.*  
694 *tabacum*, also made them good candidates for this assay. Interestingly, DsEcp20-3, like DsEcp32-3,  
695 was able to trigger a cell death response in all pine genotypes tested. Taken together, these results  
696 suggest that the DsEcp20-3 and DsEcp32-3 proteins could also be recognized by an immune receptor  
697 (possibly conserved with *N. benthamiana*) or, as described above, participate in membrane  
698 perturbation in *P. radiata*. Consistent with what was observed in the non-host plants, DsEcp20-4 was  
699 unable to elicit a cell death response in the pine shoots. This may suggest that it does not have the  
700 conserved epitope required to elicit cell death following recognition by an immune receptor. To  
701 identify the regions or amino acid residues involved in cell death induction, and thus potential  
702 epitopes for recognition by cognate immune receptors, region swaps between cell death-eliciting and  
703 non-eliciting members of the Ecp20 and Ecp32 families, based on information gained from the  
704 prediction of surface-exposed residues by AlphaFold2, can now be performed in *Nicotiana* species or  
705 pine, similar to that described for the Avr4 effector protein of *D. septosporum* and *F. fulva* in *N.*  
706 *benthamiana* (Mesarich et al., 2016). This, in turn, might help to explain the differences in cell death-  
707 inducing capacity between, for example, CfEcp32-1 and DsEcp32-1, as well as DsEcp20-3 and  
708 DsEcp20-4.

709 As it is well known that plant cell death is a strategy exploited by necrotrophic and hemibiotrophic  
710 pathogens to acquire nutrients from their hosts during their necrotrophic stage or to facilitate a  
711 biotrophic–necrotrophic switch (Shao et al., 2021), one possibility is that the DsEcp20-3 and  
712 DsEcp32-3 proteins from *D. septosporum* are involved in these processes. In addition to their cell  
713 death-eliciting activities, support for this hypothesis is provided by the fact that the expression of  
714 both *DsEcp20-3* and *DsEcp32-3* is highly induced during the Mid and Late stages of pine infection  
715 by *D. septosporum*. Another possibility is that DsEcp20-3 may be acting as an Avr factor of *D.*  
716 *septosporum* recognized by the host, similar to that already proposed for the core effector DsEcp2-1  
717 (Guo et al., 2020), while other family members, such as DsEcp20-4, which is also highly expressed  
718 during pine infection, might be virulence factors that interact with pine PR5 proteins to suppress host  
719 defenses. One way to approach these research questions is to generate mutants of *D. septosporum*  
720 deleted for a *DsEcp20* or *DsEcp32* gene (e.g., using CRISPR/Cas9 technology) to determine what  
721 impact their deletion or disruption has on necrotrophic infection by this fungus. The problem with  
722 this method is that because these genes form part of multigene families, functional redundancy may  
723 mask the role of the individual effectors (i.e. the deletion mutants may not show a reduction in  
724 virulence). However, it may be possible to create strains in which genes corresponding to several or  
725 all family members are deleted to assess whether fungal virulence, particularly in the necrotrophic  
726 infection stage, is compromised. Recently, we reported the first successful application of  
727 CRISPR/Cas9 genome editing to *D. septosporum* by disrupting a gene encoding a secreted protein  
728 that elicited cell death in *N. benthamiana* and pine (McCarthy et al., 2022), which will ultimately  
729 help with creating such strains.

730 In conclusion, our study describes two new candidate effector families with cell death-eliciting  
731 activity from *D. septosporum* and *F. fulva* and provides evidence to suggest that members of these  
732 families are recognized as invasion patterns by immune receptors of phylogenetically distinct plant  
733 species (angiosperms versus a gymnosperm). By characterizing the virulence (and potential  
734 avirulence) functions of such ‘core’ effectors, the knowledge gained could ultimately be used in  
735 durable disease resistance programs active against these two, and other, important plant pathogens.

736 **5 Conflict of Interest**

737 The authors declare that the research was conducted in the absence of any commercial or financial  
738 relationships that could be construed as a potential conflict of interest.

739 **6 Author Contributions**

740 R.B., R.M., Y.W. and C.M. conceived and guided the study. M.T. and Z.C. designed and performed  
741 experiments and analyzed data. M.T., C.M. and R.B. led manuscript writing. All authors contributed  
742 to the manuscript.

743 **7 Funding**

744 This research was funded by Scion (New Zealand Forest Research Institute, Ltd., Rotorua, New  
745 Zealand) and through the Resilient Forests Research Program via Strategic Science Investment  
746 Funding from the New Zealand Ministry of Business Innovation and Employment (MBIE), grant  
747 number CO4X1703, and New Zealand Forest Grower Levy Trust funding, grant number QT-9108.

748 **8 Acknowledgments**

749 We thank Melissa Guo (Massey University, Palmerston North, New Zealand) and Lukas Hunziker  
750 (Curtin University, Perth, Australia) for input on experiments. Trevor S. Loo (Massey University,  
751 Palmerston North, New Zealand) is acknowledged for his advice on performing the IMAC, and  
752 Keiko Gough (Scion, Rotorua, New Zealand) for preparing the pine material.

753 **9 References**

- 754 Anderson, C., Khan, M. A., Catanzariti, A.-M., Jack, C. A., Nemri, A., Lawrence, G. J., Upadhyaya,  
755 N. M., Hardham, A. R., Ellis, J. G., Dodds, P. N. & Jones, D. A. (2016). Genome analysis and  
756 avirulence gene cloning using a high-density RADseq linkage map of the flax rust fungus,  
757 *Melampsora lini*. *BMC Genom.*, 17(1), 1-20. doi: 10.1186/s12864-016-3011-9
- 758 Barnes, I., Crous, P. W., Wingfield, B. D. & Wingfield, M. J. (2004). Multigene phylogenies reveal  
759 that red band needle blight of *Pinus* is caused by two distinct species of *Dothistroma*, *D.*  
760 *septosporum* and *D. pini*. *Stud. Mycol.*, 50(2), 551-565.
- 761 Bolton, M. D., Van Esse, H. P., Vossen, J. H., De Jonge, R., Stergiopoulos, I., Stulemeijer, I. J. E.,  
762 Van Den Berg, G. C. M., Borrás-Hidalgo, O., Dekker, H. L., De Koster, C. G., De Wit, P. J.  
763 G. M., Joosten, M. H. A. J. & Thomma, B. P. H. J. (2008). The novel *Cladosporium fulvum*  
764 lysis motif effector Ecp6 is a virulence factor with orthologues in other fungal species. *Mol.*  
765 *Microbiol.*, 69(1), 119-136. doi: 10.1111/j.1365-2958.2008.06270.x
- 766 Bradshaw, R. E., Guo, Y., Sim, A. D., Kabir, M. S., Chettri, P., Ozturk, I. K., Hunziker, L., Ganley,  
767 R. J. & Cox, M. P. (2016). Genome-wide gene expression dynamics of the fungal pathogen  
768 *Dothistroma septosporum* throughout its infection cycle of the gymnosperm host *Pinus*  
769 *radiata*. *Mol. Plant Pathol.*, 17(2), 210-224. doi: 10.1111/mpp.12273
- 770 Bradshaw, R. E., Sim, A. D., Chettri, P., Dupont, P.-Y., Guo, Y., Hunziker, L., McDougal, R. L.,  
771 Van der Nest, A., Fourie, A., Wheeler, D., Cox, M. P. & Barnes, I. (2019). Global population  
772 genomics of the forest pathogen *Dothistroma septosporum* reveal chromosome duplications  
773 in high dothistromin-producing strains. *Mol. Plant Pathol.*, 20(6), 784-799. doi:  
774 10.1111/mpp.12791

- 775 Catanzariti, A.-M., Dodds, P. N., Lawrence, G. J., Ayliffe, M. A. & Ellis, J. G. (2006). Haustorially  
776 expressed secreted proteins from flax rust are highly enriched for avirulence elicitors. *Plant*  
777 *Cell*, 18(1), 243-256. doi: 10.1105/tpc.105.035980
- 778 Chruszcz, M., Chapman, M. D., Osinski, T., Solberg, R., Demas, M., Porebski, P. J., Majorek, K. A.,  
779 Pomés, A. & Minor, W. (2012). *Alternaria alternata* allergen Alt a 1: a unique  $\beta$ -barrel  
780 protein dimer found exclusively in fungi. *J. Allergy Clin. Immunol.*, 130(1), 241-247. doi:  
781 10.1016/j.jaci.2012.03.047
- 782 Coll, N. S., Epple, P. & Dangl, J. L. (2011). Programmed cell death in the plant immune system. *Cell*  
783 *Death Differ.*, 18(8), 1247-1256. doi: 10.1038/cdd.2011.37
- 784 Cook, D. E., Mesarich, C. H. & Thomma, B. P. H. J. (2015). Understanding plant immunity as a  
785 surveillance system to detect invasion. *Annu. Rev. Phytopathol.*, 53(1), 541-563. doi:  
786 10.1146/annurev-phyto-080614-120114
- 787 de Jonge, R., Peter van Esse, H., Kombrink, A., Shinya, T., Desaki, Y., Bours, R., van der Krol, S.,  
788 Shibuya, N., Joosten Matthieu, H. A. J. & Thomma Bart, P. H. J. (2010). Conserved fungal  
789 LysM effector Ecp6 prevents chitin-triggered immunity in plants. *Science*, 329(5994), 953-  
790 955. doi: 10.1126/science.1190859
- 791 de Wit, P. J. (2016). *Cladosporium fulvum* effectors: weapons in the arms race with tomato. *Annu.*  
792 *Rev. Phytopathol.*, 54(1), 1-23. doi: 10.1146/annurev-phyto-011516-040249
- 793 de Wit, P. J., van der Burgt, A., Okmen, B., Stergiopoulos, I., Abd-Elsalam, K. A., Aerts, A. L.,  
794 Bahkali, A. H., Beenen, H. G., Chettri, P., Cox, M. P., Datema, E., de Vries, R. P., Dhillon,  
795 B., Ganley, A. R., Griffiths, S. A., Guo, Y., Hamelin, R. C., Henrissat, B., Kabir, M. S.,  
796 Jashni, M. K., Kema, G., Klaubauf, S., Lapidus, A., Levasseur, A., Lindquist, E., Mehrabi, R.,  
797 Ohm, R. A., Owen, T. J., Salamov, A., Schwelm, A., Schijlen, E., Sun, H., van den Burg, H.  
798 A., van Ham, R. C., Zhang, S., Goodwin, S. B., Grigoriev, I. V., Collemare, J. & Bradshaw,  
799 R. E. (2012). The genomes of the fungal plant pathogens *Cladosporium fulvum* and  
800 *Dothistroma septosporum* reveal adaptation to different hosts and lifestyles but also  
801 signatures of common ancestry. *PLoS Genet.*, 8(11), e1003088. doi:  
802 10.1371/journal.pgen.1003088
- 803 DeLano, W. L. (2002). Pymol: an open-source molecular graphics tool. *CCP4 Newslett. Protein*  
804 *Crystallogr.*, 40(1), 82-92.
- 805 Deng, C. H., Plummer, K. M., Jones, D. A. B., Mesarich, C. H., Shiller, J., Taranto, A. P., Robinson,  
806 A. J., Kastner, P., Hall, N. E., Templeton, M. D. & Bowen, J. K. (2017). Comparative  
807 analysis of the predicted secretomes of Rosaceae scab pathogens *Venturia inaequalis* and *V.*  
808 *pirina* reveals expanded effector families and putative determinants of host range. *BMC*  
809 *Genom.*, 18(1), 339. doi: 10.1186/s12864-017-3699-1
- 810 Denton-Giles, M., McCarthy, H., Sehrish, T., Dijkwel, Y., Mesarich, C. H., Bradshaw, R. E., Cox,  
811 M. P. & Dijkwel, P. P. (2020). Conservation and expansion of a necrosis-inducing small  
812 secreted protein family from host-variable phytopathogens of the Sclerotiniaceae. *Mol. Plant*  
813 *Pathol.*, 21(4), 512-526. doi: 10.1111/mpp.12913
- 814 Dodds, P. N., Lawrence, G. J., Catanzariti, A.-M., Ayliffe, M. A. & Ellis, J. G. (2004). The  
815 *Melampsora lini* AvrL567 avirulence genes are expressed in haustoria and their products are  
816 recognized inside plant cells. *Plant Cell*, 16(3), 755-768. doi: 10.1105/tpc.020040
- 817 Dong, Y., Burch-Smith, T. M., Liu, Y., Mamillapalli, P. & Dinesh-Kumar, S. P. (2007). A ligation-  
818 independent cloning tobacco rattle virus vector for high-throughput virus-induced gene

- 819 silencing identifies roles for NbMADS4-1 and -2 in Floral Development. *Plant Physiol.*,  
820 145(4), 1161-1170. doi: 10.1104/pp.107.107391
- 821 Doyle, J. J. & Doyle, J. L. (1987). A rapid DNA isolation procedure for small quantities of fresh leaf  
822 tissue. *Phytochem. Bull.*, 19, 11-15.
- 823 Drenkhan, R., Tomešová-Haataja, V., Fraser, S., Bradshaw, R. E., Vahalík, P., Mullett, M. S.,  
824 Martín-García, J., Bulman, L. S., Wingfield, M. J., Kirisits, T., Cech, T. L., Schmitz, S.,  
825 Baden, R., Tubby, K., Brown, A., Georgieva, M., Woods, A., Ahumada, R., Jankovský, L.,  
826 Thomsen, I. M., Adamson, K., Marçais, B., Vuorinen, M., Tsopelas, P., Koltay, A., Halasz, A.,  
827 La Porta, N., Anselmi, N., Kiesnere, R., Markovskaja, S., Kačergius, A., Papazova-  
828 Anakieva, I., Risteski, M., Sotirovski, K., Lazarević, J., Solheim, H., Boroň, P., Bragança, H.,  
829 Chira, D., Musolin, D. L., Selikhovkin, A. V., Bulgakov, T. S., Keča, N., Karadžić, D.,  
830 Galovic, V., Pap, P., Markovic, M., Poljakovic Pajnik, L., Vasic, V., Ondrušková, E., Piškur, B.,  
831 Sadiković, D., Diez, J. J., Solla, A., Millberg, H., Stenlid, J., Angst, A., Queloz, V.,  
832 Lehtijärvi, A., Doğmuş-Lehtijärvi, H. T., Oskay, F., Davydenko, K., Meshkova, V., Craig, D.,  
833 Woodward, S. & Barnes, I. (2016). Global geographic distribution and host range of  
834 *Dothistroma* species: a comprehensive review. *For. Pathol.*, 46(5), 408-442. doi:  
835 10.1111/efp.12290
- 836 Engler, C., Gruetzner, R., Kandzia, R. & Marillonnet, S. (2009). Golden Gate Shuffling: A one-pot  
837 DNA shuffling method based on type IIIs restriction enzymes. *PLoS One*, 4(5), e5553. doi:  
838 10.1371/journal.pone.0005553
- 839 Fellbrich, G., Romanski, A., Varet, A., Blume, B., Brunner, F., Engelhardt, S., Felix, G.,  
840 Kemmerling, B., Krzymowska, M. & Nürnberg, T. (2002). NPP1, a *Phytophthora*-  
841 associated trigger of plant defense in parsley and *Arabidopsis*. *Plant J.*, 32(3), 375-390. doi:  
842 10.1046/j.1365-313X.2002.01454.x
- 843 Franceschetti, M., Maqbool, A., Jiménez-Dalmaroni, M. J., Pennington, H. G., Kamoun, S. &  
844 Banfield, M. J. (2017). Effectors of filamentous plant pathogens: commonalities amid  
845 diversity. *Microbiol. Mol. Biol. Rev.*, 81(2), e00066. doi: 10.1128/MMBR.00066-16
- 846 Gómez-Casado, C., Murua-García, A., Garrido-Arandia, M., González-Melendi, P., Sánchez-Monge,  
847 R., Barber, D., Pacios, L. F. & Díaz-Perales, A. (2014). Alt a 1 from *Alternaria* interacts with  
848 PR5 thaumatin-like proteins. *FEBS Lett.*, 588(9), 1501-1508. doi:  
849 10.1016/j.febslet.2014.02.044
- 850 Guo, Y., Hunziker, L., Mesarich, C. H., Chettri, P., Dupont, P.-Y., Ganley, R. J., McDougal, R. L.,  
851 Barnes, I. & Bradshaw, R. E. (2020). DsEcp2-1 is a polymorphic effector that restricts growth  
852 of *Dothistroma septosporum* in pine. *Fungal Genet. and Biol.*, 135, 103300. doi:  
853 10.1016/j.fgb.2019.103300
- 854 Han, L., Liu, Z., Liu, X. & Qiu, D. (2012). Purification, crystallization and preliminary X-ray  
855 diffraction analysis of the effector protein PevD1 from *Verticillium dahliae*. *Acta Crystallogr.*  
856 *F: Struct. Biol. Commun.*, 68(7), 802-805. doi: 10.1107/S1744309112020556
- 857 Hargreaves, C., Grace, L., Maas, S. v. d., Reeves, C., Holden, G., Menzies, M., Kumar, S. & Foggo,  
858 M. (2004). Cryopreservation of *Pinus radiata* zygotic embryo cotyledons: effect of storage  
859 duration on adventitious shoot formation and plant growth after 2 years in the field. *Can. J.  
860 For. Res.*, 34(3), 600-608. doi: 10.1139/x03-226
- 861 Heese, A., Hann Dagmar, R., Gimenez-Ibanez, S., Jones Alexandra, M. E., He, K., Li, J., Schroeder  
862 Julian, I., Peck Scott, C. & Rathjen John, P. (2007). The receptor-like kinase SERK3/BAK1 is

- 863 a central regulator of innate immunity in plants. *PNAS*, 104(29), 12217-12222. doi:  
864 10.1073/pnas.0705306104
- 865 Holm, L. (2020). "Using Dali for Protein Structure Comparison," in *Structural Bioinformatics: Methods and Protocols*, ed. Z. Gáspári (New York, NY: Springer US), 29-42. doi:  
866 10.1007/978-1-0716-0270-6-3
- 867 Holsters, M., Silva, B., Van Vliet, F., Genetello, C., De Block, M., Dhaese, P., Depicker, A., Inzé, D.,  
868 Engler, G., Villarroel, R., Van Montagu, M. & Schell, J. (1980). The functional organization  
869 of the nopaline *A. tumefaciens* plasmid pTiC58. *Plasmid*, 3(2), 212-230. doi: 10.1016/0147-  
870 619X(80)90110-9
- 871 Hunziker, L., Tarallo, M., Gough, K., Guo, M., Hargreaves, C., Loo, T. S., McDougal, R. L.,  
872 Mesarich, C. H. & Bradshaw, R. E. (2021). Apoplastic effector candidates of a foliar forest  
873 pathogen trigger cell death in host and non-host plants. *Sci. Rep.*, 11(1), 19958. doi:  
874 10.1038/s41598-021-99415-5
- 875 Jones, J. D. G. & Dangl, J. L. (2006). The plant immune system. *Nature*, 444(7117), 323-329. doi:  
876 10.1038/nature05286
- 877 Juillot, S., Cott, C., Madl, J., Claudinon, J., van der Velden, N. S. J., Künzler, M., Thuenauer, R. &  
878 Römer, W. (2016). Uptake of *Marasmius oreades* agglutinin disrupts integrin-dependent cell  
879 adhesion. *Biochim. Biophys. Acta*, 1860(2), 392-401. doi: 10.1016/j.bbagen.2015.11.002
- 880 Jumper, J., Evans, R., Pritzel, A., Green, T., Figurnov, M., Ronneberger, O., Tunyasuvunakool, K.,  
881 Bates, R., Žídek, A., Potapenko, A., Bridgland, A., Meyer, C., Kohl, S. A. A., Ballard, A. J.,  
882 Cowie, A., Romera-Paredes, B., Nikolov, S., Jain, R., Adler, J., Back, T., Petersen, S.,  
883 Reiman, D., Clancy, E., Zielinski, M., Steinegger, M., Pacholska, M., Berghammer, T.,  
884 Bodenstein, S., Silver, D., Vinyals, O., Senior, A. W., Kavukcuoglu, K., Kohli, P. &  
885 Hassabis, D. (2021). Highly accurate protein structure prediction with AlphaFold. *Nature*,  
886 596(7873), 583-589. doi: 10.1038/s41586-021-03819-2
- 887 Kabir, M. S., Ganley, R. J. & Bradshaw, R. E. (2015). The hemibiotrophic lifestyle of the fungal pine  
888 pathogen *Dothistroma septosporum*. *For. Pathol.*, 45(3), 190-202. doi: 10.1111/efp.12153
- 889 Kamoun, S., van West, P., de Jong, A. J., de Groot, K. E., Vleeshouwers, V. G. A. A. & Govers, F.  
890 (1997). A gene encoding a protein elicitor of *Phytophthora infestans* is down-regulated during  
891 infection of potato. *Mol. Plant Microbe Interact.*, 10(1), 13-20. doi:  
892 10.1094/mpmi.1997.10.1.13
- 893 Kang, S., Sweigard, J. A. & Valent, B. (1995). The PWL host specificity gene family in the blast  
894 fungus *Magnaporthe grisea*. *Mol. Plant Microbe Interact.*, 8(6), 939-948. doi: 10.1094/mpmi-  
895 8-0939
- 896 Kanzaki, H., Saitoh, H., Takahashi, Y., Berberich, T., Ito, A., Kamoun, S. & Terauchi, R. (2008).  
897 NbLRK1, a lectin-like receptor kinase protein of *Nicotiana benthamiana*, interacts with  
898 *Phytophthora infestans* INF1 elicitin and mediates INF1-induced cell death. *Planta*, 228(6),  
899 977-987. doi: 10.1007/s00425-008-0797-y
- 900 Kearse, M., Moir, R., Wilson, A., Stones-Havas, S., Cheung, M., Sturrock, S., Buxton, S., Cooper,  
901 A., Markowitz, S., Duran, C., Thierer, T., Ashton, B., Meintjes, P. & Drummond, A. (2012).  
902 Geneious basic: an integrated and extendable desktop software platform for the organization  
903 and analysis of sequence data. *Bioinformatics*, 28(12), 1647-1649. doi:  
904 10.1093/bioinformatics/bts199
- 905

- 906 Kettles, G. J., Bayon, C., Canning, G., Rudd, J. J. & Kanyuka, K. (2017). Apoplastic recognition of  
907 multiple candidate effectors from the wheat pathogen *Zymoseptoria tritici* in the nonhost  
908 plant *Nicotiana benthamiana*. *New Phytol.*, 213(1), 338-350. doi: 10.1111/nph.14215
- 909 Khang, C. H., Park, S.-Y., Lee, Y.-H., Valent, B. & Kang, S. (2008). Genome organization and  
910 evolution of the AVR-Pita avirulence gene family in the *Magnaporthe grisea* species  
911 complex. *Mol. Plant Microbe Interact.*, 21(5), 658-670. doi: 10.1094/mpmi-21-5-0658
- 912 Kombrink, A. (2012). "Heterologous production of fungal effectors in *Pichia pastoris*," in Plant  
913 Fungal Pathogens: Methods and Protocols, ed. M. D. Bolton & B. P. H. J. Thomma (Totowa,  
914 NJ: Humana Press), 209-217. doi: 10.1007/978-1-61779-501-5-13
- 915 Kumar, R. & Mukherjee, P. K. (2020). *Trichoderma virens* Alt a 1 protein may target maize  
916 PR5/thaumatin-like protein to suppress plant defence: an in silico analysis. *Physiol. Mol.*  
917 *Plant Pathol.*, 112, 101551. doi: 10.1016/j.pmpp.2020.101551
- 918 Liebrand, T. W. H., van den Berg Grardy, C. M., Zhang, Z., Smit, P., Cordewener Jan, H. G.,  
919 America Antoine, H. P., Sklenar, J., Jones Alexandra, M. E., Tameling Wladimir, I. L.,  
920 Robatzek, S., Thomma Bart, P. H. J. & Joosten Matthieu, H. A. J. (2013). Receptor-like  
921 kinase SOBIR1/EVR interacts with receptor-like proteins in plant immunity against fungal  
922 infection. *PNAS*, 110(24), 10010-10015. doi: 10.1073/pnas.1220015110
- 923 Liebrand, T. W. H., van den Burg, H. A. & Joosten, M. H. A. J. (2014). Two for all: receptor-  
924 associated kinases SOBIR1 and BAK1. *Trends Plant Sci.*, 19(2), 123-132. doi:  
925 10.1016/j.tplants.2013.10.003
- 926 Liu, Y., Schiff, M., Marathe, R. & Dinesh-Kumar, S. P. (2002). Tobacco *Rar1*, *EDS1* and  
927 *NPRI/NIM1* like genes are required for N-mediated resistance to tobacco mosaic virus. *Plant*  
928 *J.*, 30(4), 415-429. doi: 10.1046/j.1365-313X.2002.01297.x
- 929 Livak, K. J. & Schmittgen, T. D. (2001). Analysis of relative gene expression data using real-time  
930 quantitative PCR and the 2- $\Delta\Delta CT$  method. *Methods*, 25(4), 402-408. doi:  
931 10.1006/meth.2001.1262
- 932 Lo Presti, L., Lanver, D., Schweizer, G., Tanaka, S., Liang, L., Tollot, M., Zuccaro, A., Reissmann,  
933 S. & Kahmann, R. (2015). Fungal effectors and plant susceptibility. *Annu. Rev. Plant. Biol.*,  
934 66, 513-545. doi: 10.1146/annurev-arplant-043014-114623
- 935 Ma, Z., Song, T., Zhu, L., Ye, W., Wang, Y., Shao, Y., Dong, S., Zhang, Z., Dou, D., Zheng, X.,  
936 Tyler, B. M. & Wang, Y. (2015). A *Phytophthora sojae* glycoside hydrolase 12 protein is a  
937 major virulence factor during soybean infection and is recognized as a PAMP. *Plant Cell*,  
938 27(7), 2057. doi: 10.1105/tpc.15.00390
- 939 MacFarlane, S. A. (1999). Molecular biology of the tobaviruses. *J. Gen. Virol.*, 80(11), 2799-2807.  
940 doi: 10.1099/0022-1317-80-11-2799
- 941 McCarthy, H. M., Tarallo, M., Mesarich, C. H., McDougal, R. L. & Bradshaw, R. E. (2022).  
942 Targeted gene mutations in the forest pathogen *Dothistroma septosporum* using  
943 CRISPR/Cas9. *Plants*, 11(8) doi: 10.3390/plants11081016
- 944 Mesarich, C. H., Stergiopoulos, I., Beenen, H. G., Cordovez, V., Guo, Y., Karimi Jashni, M.,  
945 Bradshaw, R. E. & de Wit, P. J. G. M. (2016). A conserved proline residue in  
946 Dothideomycete Avr4 effector proteins is required to trigger a Cf-4-dependent hypersensitive  
947 response. *Mol. Plant Pathol.*, 17(1), 84-95. doi: 10.1111/mpp.12265

- 948 Mesarich, C. H., Okmen, B., Rovenich, H., Griffiths, S. A., Wang, C., Karimi Jashni, M.,  
949 Mihajlovski, A., Collemare, J., Hunziker, L. & Deng, C. H. (2018). Specific hypersensitive  
950 response-associated recognition of new apoplastic effectors from *Cladosporium fulvum* in  
951 wild tomato. *Mol. Plant Microbe Interact.*, 31(1), 145-162. doi: 10.1094/mpmi-05-17-0114-  
952 FI
- 953 Mirdita, M., Schütze, K., Moriwaki, Y., Heo, L., Ovchinnikov, S. & Steinegger, M. (2022).  
954 ColabFold: making protein folding accessible to all. *Nat. Methods*. doi: 10.1038/s41592-022-  
955 01488-1
- 956 Mueller, A. N., Ziemann, S., Treitschke, S., Aßmann, D. & Doeblemann, G. (2013). Compatibility in  
957 the *Ustilago maydis*-maize interaction requires inhibition of host cysteine proteases by the  
958 fungal effector Pit2. *PLoS Pathog.*, 9(2), e1003177. doi: 10.1371/journal.ppat.1003177
- 959 Nürnberger, T. & Brunner, F. (2002). Innate immunity in plants and animals: emerging parallels  
960 between the recognition of general elicitors and pathogen-associated molecular patterns.  
961 *Curr. Opin. Plant Biol.*, 5(4), 318-324. doi: 10.1016/S1369-5266(02)00265-0
- 962 Pendleton, A. L., Smith, K. E., Feau, N., Martin, F. M., Grigoriev, I. V., Hamelin, R., Nelson, C. D.,  
963 Burleigh, J. G. & Davis, J. M. (2014). Duplications and losses in gene families of rust  
964 pathogens highlight putative effectors. *Front. Plant Sci.*, 5(299). doi:  
965 10.3389/fpls.2014.00299
- 966 Praz, C. R., Bourras, S., Zeng, F., Sánchez-Martín, J., Menardo, F., Xue, M., Yang, L., Roffler, S.,  
967 Böni, R., Herren, G., McNally, K. E., Ben-David, R., Parlange, F., Oberhaensli, S., Flückiger,  
968 S., Schäfer, L. K., Wicker, T., Yu, D. & Keller, B. (2017). AvrPm2 encodes an RNase-like  
969 avirulence effector which is conserved in the two different specialized forms of wheat and rye  
970 powdery mildew fungus. *New Phytol.*, 213(3), 1301-1314. doi: 10.1111/nph.14372
- 971 Renko, M., Sabotič, J. & Turk, D. (2012).  $\beta$ -Trefoil inhibitors – from the work of Kunitz onward.  
972 *Biol. Chem.*, 393(10), 1043-1054. doi:10.1515/hsz-2012-0159
- 973 Rocafort, M., Bowen, J. K., Hassing, B., Cox, M. P., McGreal, B., de la Rosa, S., Plummer, K. M.,  
974 Bradshaw, R. E. & Mesarich, C. H. (2022). The *Venturia inaequalis* effector repertoire is  
975 expressed in waves, and is dominated by expanded families with predicted structural  
976 similarity to avirulence proteins from other fungi. *bioRxiv*, 2022.2003.2022.482717. doi:  
977 10.1101/2022.03.22.482717
- 978 Rocafort, M., Fudal, I. & Mesarich, C. H. (2020). Apoplastic effector proteins of plant-associated  
979 fungi and oomycetes. *Curr. Opin. Plant Biol.*, 56, 9-19. doi: 10.1016/j.pbi.2020.02.004
- 980 Sabotič, J., Renko, M. & Kos, J. (2019).  $\beta$ -Trefoil protease inhibitors unique to higher fungi. *Acta*  
981 *Chim. Slov.*, 66(1). doi: 10.17344/acsi.2018.4465
- 982 Sánchez-Vallet, A., Saleem-Batcha, R., Kombrink, A., Hansen, G., Valkenburg, D.-J., Thomma, B.  
983 P. H. J. & Mesters, J. R. (2013). Fungal effector Ecp6 outcompetes host immune receptor for  
984 chitin binding through intrachain LysM dimerization. *eLife*, 2, e00790. doi:  
985 10.7554/eLife.00790
- 986 Schubert, M., Bleuler-Martinez, S., Butschi, A., Wälti, M. A., Egloff, P., Stutz, K., Yan, S., Collot,  
987 M., Mallet, J.-M., Wilson, I. B. H., Hengartner, M. O., Aebi, M., Allain, F. H. T. & Künzler,  
988 M. (2012). Plasticity of the  $\beta$ -trefoil protein fold in the recognition and control of invertebrate  
989 predators and parasites by a fungal defence system. *PLoS Pathog.*, 8(5), e1002706. doi:  
990 10.1371/journal.ppat.1002706

- 991 Seong, K. & Krasileva, K. V. (2022). Comparative computational structural genomics highlights  
992 divergent evolution of fungal effectors. *bioRxiv*, 2022.2005.2002.490317. doi:  
993 10.1101/2022.05.02.490317
- 994 Shao, D., Smith, D. L., Kabbage, M. & Roth, M. G. (2021). Effectors of plant necrotrophic fungi.  
995 *Front. Plant Sci.*, 12. doi: 10.3389/fpls.2021.687713
- 996 Sharon, N. (2007). Lectins: carbohydrate-specific reagents and biological recognition molecules. *The*  
997 *J. Biol. Chem.*, 282(5), 2753-2764. doi: 10.1074/jbc.X600004200
- 998 Sievers, F., Wilm, A., Dineen, D., Gibson, T. J., Karplus, K., Li, W., Lopez, R., McWilliam, H.,  
999 Remmert, M., Söding, J., Thompson, J. D. & Higgins, D. G. (2011). Fast, scalable generation  
1000 of high-quality protein multiple sequence alignments using Clustal Omega. *Mol. Syst. Biol.*, 7,  
1001 539-539. doi: 10.1038/msb.2011.75
- 1002 Soberón, M., López-Díaz, J. A. & Bravo, A. (2013). Cyt toxins produced by *Bacillus thuringiensis*: a  
1003 protein fold conserved in several pathogenic microorganisms. *Peptides*, 41, 87-93. doi:  
1004 10.1016/j.peptides.2012.05.023
- 1005 Spanu, P. D. (2017). Cereal immunity against powdery mildews targets RNase-Like proteins  
1006 associated with haustoria (RALPH) effectors evolved from a common ancestral gene. *New*  
1007 *Phytol.*, 213(3), 969-971. doi: 10.1111/nph.14386
- 1008 Sperschneider, J. & Dodds, P. N. (2021). EffectorP 3.0: prediction of apoplastic and cytoplasmic  
1009 effectors in fungi and oomycetes. *bioRxiv*, 2021.2007.2028.454080. doi:  
1010 10.1101/2021.07.28.454080
- 1011 Stergiopoulos, I., Kourmpetis, Y. A. I., Slot, J. C., Bakker, F. T., De Wit, P. J. G. M. & Rokas, A.  
1012 (2012). In silico characterization and molecular evolutionary analysis of a novel superfamily  
1013 of fungal effector proteins. *Mol. Biol. Evol.*, 29(11), 3371-3384. doi: 10.1093/molbev/mss143
- 1014 Stergiopoulos, I., van den Burg, H. A., Ökmen, B., Beenen, H. G., van Liere, S., Kema, G. H. J. & de  
1015 Wit, P. J. G. M. (2010). Tomato Cf resistance proteins mediate recognition of cognate  
1016 homologous effectors from fungi pathogenic on dicots and monocots. *PNAS*, 107(16), 7610.  
1017 doi: 10.1073/pnas.1002910107
- 1018 Talbi, N., Fokkens, L., Audran, C., Petit-Houdenot, Y., Pouzet, C., Blaise, F., Gay, E., Rouxel, T.,  
1019 Balesdent, M.-H., Rep, M. & Fudal, I. (2022). The neighboring genes *AvrLm10A* and  
1020 *AvrLm10B* are part of a large multigene family of cooperating effector genes conserved in  
1021 Dothideomycetes and Sordariomycetes. *bioRxiv*, 2022.2005.2010.491286. doi:  
1022 10.1101/2022.05.10.491286
- 1023 Taylor, R. G., Walker, D. C. & McInnes, R. R. (1993). *E. coli* host strains significantly affect the  
1024 quality of small scale plasmid DNA preparations used for sequencing. *Nucleic Acids Res.*,  
1025 21(7), 1677-1678. doi: 10.1093/nar/21.7.1677
- 1026 Thomma, B. P. H. J., Van Esse, H. P., Crous, P. W. & De Wit, P. J. G. M. (2005). *Cladosporium*  
1027 *fulvum* (syn. *Passalora fulva*), a highly specialized plant pathogen as a model for functional  
1028 studies on plant pathogenic Mycosphaerellaceae. *Mol. Plant Pathol.*, 6(4), 379-393. doi:  
1029 10.1111/j.1364-3703.2005.00292.x
- 1030 Tian, M., Win, J., Song, J., van der Hoorn, R., van der Knaap, E. & Kamoun, S. (2007). A  
1031 *Phytophthora infestans* cystatin-like protein targets a novel tomato papain-like apoplastic  
1032 protease. *Plant Physiol.*, 143(1), 364-377. doi: 10.1104/pp.106.090050

- 1033 Untergasser, A., Cutcutache, I., Koressaar, T., Ye, J., Faircloth, B. C., Remm, M. & Rozen, S. G.  
1034 (2012). Primer3 - new capabilities and interfaces. *Nucleic Acids Res.*, 40(15), e115. doi:  
1035 10.1093/nar/gks596
- 1036 van den Burg, H., Harrison, S., Joosten, M., Vervoort, J. & de Wit, P. (2006). *Cladosporium fulvum*  
1037 Avr4 protects fungal cell walls against hydrolysis by plant chitinases accumulating during  
1038 infection. *Mol. Plant Microbe Interact.*, 19(12), 1420-1430. doi: 10.1094/mpmi-19-1420
- 1039 van Esse, H. P., Van't Klooster, J. W., Bolton, M. D., Yadeta, K. A., van Baarlen, P., Boeren, S.,  
1040 Vervoort, J., de Wit, P. J. G. M. & Thomma, B. P. H. J. (2008). The *Cladosporium fulvum*  
1041 virulence protein Avr2 inhibits host proteases required for basal defense. *Plant Cell*, 20(7),  
1042 1948-1963. doi: 10.1105/tpc.108.059394
- 1043 Varrot, A., Basheer, S. M. & Imbert, A. (2013). Fungal lectins: structure, function and potential  
1044 applications. *Curr. Opin. Struct. Biol.*, 23(5), 678-685. doi: 10.1016/j.sbi.2013.07.007
- 1045 Wang, Y., Wang, Y. & Wang, Y. (2020). Apoplastic proteases: powerful weapons against pathogen  
1046 infection in plants. *Plant Commun.*, 1(4), 100085. doi: 10.1016/j.xplc.2020.100085
- 1047 Wang, Y., Xu, Y., Sun, Y., Wang, H., Qi, J., Wan, B., Ye, W., Lin, Y., Shao, Y., Dong, S., Tyler, B.  
1048 M. & Wang, Y. (2018). Leucine-rich repeat receptor-like gene screen reveals that *Nicotiana*  
1049 RXEG1 regulates glycoside hydrolase 12 MAMP detection. *Nature Commun.*, 9(1), 594. doi:  
1050 10.1038/s41467-018-03010-8
- 1051 Weber, E., Engler, C., Gruetzner, R., Werner, S. & Marillonnet, S. (2011). A modular cloning system  
1052 for standardized assembly of multigene constructs. *PLoS One*, 6(2), e16765. doi:  
1053 10.1371/journal.pone.0016765
- 1054 Weidner, M., Taupp, M. & Hallam, S. J. (2010). Expression of recombinant proteins in the  
1055 methylotrophic yeast *Pichia pastoris*. *J. Vis. Exp.*, JoVE(36), 1862. doi: 10.3791/1862
- 1056 Win, J., Chaparro-Garcia, A., Belhaj, K., Saunders, D. G., Yoshida, K., Dong, S., Schornack, S.,  
1057 Zipfel, C., Robatzek, S., Hogenhout, S. A., & Kamoun, S. (2012). Effector biology of plant-  
1058 associated organisms: concepts and perspectives. *Cold Spring Harb. Symp. Quant. Biol.*, 77,  
1059 235-247. doi: 10.1101/sqb.2012.77.015933
- 1060 Wohlschlager, T., Butschi, A., Zurfluh, K., Vonesch, S. C., Auf dem Keller, U., Gehrig, P., Bleuler-  
1061 Martinez, S., Hengartner, M. O., Aebi, M. & Künzler, M. (2011). Nematotoxicity of  
1062 *Marasmus oreades* agglutinin (MOA) depends on glycolipid binding and cysteine protease  
1063 activity. *J. Biol. Chem.*, 286(35), 30337-30343.
- 1064 Zaccaron, A. Z., Chen, L.-H., Samaras, A. & Stergiopoulos, I. (2022). A chromosome-scale genome  
1065 assembly of the tomato pathogen *Cladosporium fulvum* reveals a compartmentalized genome  
1066 architecture and the presence of a dispensable chromosome. *Microb. Genom.*, 8(4) doi:  
1067 10.1099/mgen.0.000819
- 1068 Zhang, Y., Gao, Y., Liang, Y., Dong, Y., Yang, X. & Qiu, D. (2019). *Verticillium dahliae* PevD1, an  
1069 Alt a 1-like protein, targets cotton PR5-like protein and promotes fungal infection. *J. Exp.*  
1070 *Bot.*, 70(2), 613-626. doi: 10.1093/jxb/ery351
- 1071 Zhang, Y., Liang, Y., Dong, Y., Gao, Y., Yang, X., Yuan, J., Qiu, D. (2017). The *Magnaporthe*  
1072 *oryzae* Alt A 1-like protein MoHrip1 binds to the plant plasma membrane. *Biochem. Biophys.*  
1073 *Res. Commun.*, 492(1), 55-60. doi: 10.1016/j.bbrc.2017.08.039
- 1074 Zhou, D., Lobo, Y. A., Batista, I. F. C., Marques-Porto, R., Gustchina, A., Oliva, M. L. V. &  
1075 Wlodawer, A. (2013). Crystal structures of a plant trypsin inhibitor from *Enterolobium*

- 1076        *contortisiliquum* (EcTI) and of its complex with bovine trypsin. *PLoS One*, 8(4), e62252. doi:  
1077        10.1371/journal.pone.0062252
- 1078        Žurga, S., Pohleven, J., Kos, J. & Sabotič, J. (2015).  $\beta$ -Trefoil structure enables interactions between  
1079        lectins and protease inhibitors that regulate their biological functions. *J. Biochem.*, 158(1), 83-  
1080        90. doi: 10.1093/jb/mvv025